Eur. Phys. J. C (2025) 85:345
https://doi.org/10.1140/epjc/s10052-025-14044-w

THE EUROPEAN PHYSICAL JOURNAL C

Regular Article - Theoretical Physics

Investigating the role of new physics in semileptonic $\Upsilon(nS) \to B_c l^- \bar{\nu}_l$ weak decays

Jin-Huan Sheng[1,a], **Feng-Zi Zhou**[1], **Yuan-Yuan Li**[2], **Yuan-Guo Xu**[3]

[1] School of Physics and Engineering, Henan University of Science and Technology, Luoyang 471000, Henan, China
[2] Basic Department, Information Engineering University, Zhengzhou 450000, Henan, China
[3] College of Physics and Communication Electronic, Jiangxi Normal University, Nanchang 330022, Jiangxi, China

Received: 20 November 2024 / Accepted: 9 March 2025

Abstract Recently, the excess in the measurement of the branching fractions of $\bar{B} \to D^{(*)}\tau^-\bar{\nu}_\tau$ and $B_c \to J/\Psi\tau^-\bar{\nu}_\tau$ compared to the standard model expectation hints the existence of new physics beyond the standard model. Motivated by these inspiring anomalies, which may imply hints of new physics, as well as abundant $\Upsilon(nS)$ data samples, in this work, we perform the analysis of the semileptonic decays $\Upsilon(nS) \to B_c l^-\bar{\nu}_l (n = 1, 2, 3)$, which is also induced by $b \to c l^-\bar{\nu}_l$ transitions at the quark level, both within the standard model and beyond. Starting with the most general effective Hamiltonian relevant for the $b \to c l^-\bar{\nu}_l$ transition, we report the prediction of standard model for various observables, such as branching ratios, the ratio of branching fractions, the lepton side forward-backward asymmetries, the initial hadron and final lepton longitudinal polarization asymmetries and the convexity parameter, as well as for some new observable that is similar to lepton non-universality, $R_{B_c}(q^2)$, which is related to the processes $\Upsilon(nS) \to B_c l^-\bar{\nu}_l (n = 1, 2, 3)$. These predictions are made using transition form factors which are calculated in the Bauer Stech Wirbel framework. Using previously obtained significant fits of the new physics couplings, predictions for the q^2 dependence of different observable within various new physics scenarios are also presented. Some observable of the decay modes are sizeable and deviate significantly from their corresponding prediction of the standard model, especially in new physics scenarios with S_R coupling parameter. We hope that the corresponding investigation in this work will be testified by future experiments. Additionally, the study of the meson decays will also enhance the study of b hadron decay processes, as they provide good complementary environment for searching new physics signal.

1 Introduction

The high precision frontier research of heavy flavor physics is one of the very important goals in contemporary particle physics. Related decay processes not only involves a precise test of the Standard Model(SM) but also relates to the search for new physic (NP) beyond the SM. One approach is directly compare with experimental results to identify some important discrepancies, for example, decay constant, particle mass, and decay rate of a particular physical decay process. The another method entails researching different flavor changing weak decay processes to extract the Cabibbo–Kobayashi–Maskawa (CKM) matrix elements. The precise experimental measurements and theoretical calculations are both essential and indispensable in above two methods. Historically, experimental measurements and precise theoretical calculations are often not synchronised. The high precise theoretical calculations often provide some reference value for experimental measurements.

In last few years, the existence of NP that breaks the universality of lepton flavour in many processes induced by the $b \to c\tau^-\bar{\nu}_\tau$ transitions at the quark level has been implied by the anomalous measurements in bottom meson $\bar{B} \to D^{(*)}\tau^-\bar{\nu}_\tau$ $B_c \to J/\Psi(\eta_c)l^-\bar{\nu}_l$ [1–4], $B_s \to D_s^{(*)}(K^{(*)})l^-\bar{\nu}_l$ [5–9], $B^* \to P(V)l^-\bar{\nu}_l$ [10–17] and bottom baryon decays $\Lambda_b \to \Lambda_c(p)l^-\bar{\nu}_l$ [18–27], $\Xi_b \to \Xi_c l^-\bar{\nu}_l$ [28–30], $\Omega_b \to \Omega_c l^-\bar{\nu}_l$, $\Sigma_b \to \Sigma_c l^-\bar{\nu}_l$ [31–36]. With the discovery of the upsilon in proton-nucleus collisions at Femilab [37,38], the study about bottomonium has obtained remarkable achievement. The upsilon meson $\Upsilon(nS)$ with $(n = 1, 2, 3)$ is the spin-triplet S-wave states of bottomonium (bound state consisting of bottom quark b and antibottom quark $\bar{b}$). The meson have some common features that they all lie below the open bottom threshold and they carry the same

[a] e-mail: jinhuanwuli@126.com (corresponding author)

Published online: 27 March 2025

quantum numbers of $I^G J^{PC} = 0^0 1^{--}$ [39]. In a close analogy with the charmonium J/Ψ, $\psi(1S, 2S)$ and $\eta_c(1S, 2S)$ which predominantly decay through the strong and electromagnetic interactions, the $\Upsilon(nS)$ also occur mainly through strong, electromagnetic processes. Besides, the coupling constant for hadronic upsilon decay is smaller than the one for charmonium decay owing to the quantum chromo dynamics (QCD) asymptotic freedom. Thanks to the significant process achieved in recent years about the improvement of luminosity of colliders, a large number of rare weak decays have been observed. For instance, the decays of $\Upsilon(1S)$ and J/Ψ have been researched widely, both theoretically and experimentally. And the weak decay channels of them attract lots of attention [40–53]. Especially, the detailed study about $\Upsilon(1S) \to B_c M(M = \rho, D_s^{(*)}, \pi, K)$ weak decays with the perturbative QCD (PQCD) [54–56] approach and the QCD factorization (QCDF) [57,58] approach are done by research group of Profs. Sun and Chang. On this basis, they also further explored $\Upsilon(nS) \to B_c M(M = \rho, D_{s(d)}^{(*)}, \pi, K^{(*)}$ weak decays with PQCD and QCDF approach [59–63]. From the discussion of these references, we know that the $\Upsilon(nS)$ decays, especially, the $\Upsilon(1S)$ is dominated by the annihilation of the $b\bar{b}$ quark pairs into three gluons and the branching ratios $\mathcal{B}(\Upsilon(nS)_{n=1,2,3} \to ggg) = (81.7 \pm 0.7, 58.8 \pm 1.2, 35.7 \pm 2.6)\%$ [39]. Besides, as an essential complement to $\Upsilon(nS)$ decay modes, the weak decays of $\Upsilon(nS)$ mesons are very rare generally [40,64], and the weak decays of these mesons is also allowable within the SM.

Experimentally, there is a large number of $\Upsilon(nS)$ mesons at high luminosity dedicated bottomonium factories. So far, there is over 10^8 data samples about $\Upsilon(nS)$ that have been accumulated by the Belle detector at the KEKB and the BaBar detector at the PEP-II e^+e^- asymmetric energy colliders due to their outstanding performance [65]. Furthermore, the ATLAS, CMS and LHCb experiments also collect large number the data samples $\Upsilon(nS)$. It is hopefully expected that much more $b\bar{b}$ quark pairs will be collected with great precision at the forthcoming SuperKEKB [66] and running upgraded LHC. And large amount of data samples will provide a very good opportunity to search about the weak decay of $\Upsilon(nS)$ that in some cases may be detectable. Besides, the small branching ratios about nonleptonic two body $\Upsilon(nS) \to B_c D_{s,d}(\pi, K)$ make the observation of other upsilon weak decays more challenge experimentally. Significantly, all the possible measurements will be affected seriously from the efficiency of reconstruction and assessment of backgrounds. Furthermore, any discernible evidences of an anomalous large production rate of single B_c meson in $\Upsilon(nS)$ decays might be a sign of NP beyond the SM. It is crucial that the theoretical research about the weak decays of $\Upsilon(nS)$ and the research can also offer a ready reference. It is reasonable to investigate the similar decay process of the bottomonium in the light of the extensive search and investigation of rare charmonium from Refs. [67,68] experimentally and theoretically [41,44,69–71].

It is well known that the clear hierarchy of the quark-mixing Cabibbo-Kabayashi-Maskawa (CKM) matrix elements favors the $b \to c$ transition. The existing predictions about the semileptonic decays $\Upsilon(1S) \to B_c l^- \bar{\nu}_l$ investigated in several theoretical studies still differ. In this work, we will pay our attention to the semileptonic weak decay process $\Upsilon(nS) \to B_c l^- \bar{\nu}_l (n = 1, 2, 3)$ which are mediated by $b \to c l^- \bar{\nu}_l$ transition at the quark level in SM and various NP scenarios. Studying the decay modes not only provide an independent determination of the CKM matrix element V_{cb}, but also confirm the LFUV in R_{B_c} which have a similar formalism to $R_{D^{(*)}}$. It will draw very interesting results to investigate R_{B_c} on the decay processes $\Upsilon(nS) \to B_c \ell^- \bar{\nu}_\ell$. The complexity of the meson structures and the lack of precise predictions for various form factors may lead to variations in the prediction of different observables, such as the total decay rate Γ, the forward-backward asymmetries A_{FB}, and so on.

Studying these decay processes will facilitate significant improvements in our understanding of the processes involved. In this work, using the best fit solution for the Wilson coefficients of the new operators and the relevant the result of the form factors, we provide numerical results and contributions of NP effect on some observables that have not yet been measured, such as the differential decay rate $d\Gamma/dq^2$, the ratio of the branching fraction $\mathrm{R}_{B_c}(q^2)$, the polarization fraction of the initial meson $P_{L(T)}^{\Upsilon}(q^2)$, the lepton forward-backward asymmetry $A_{FB}^l(q^2)$, the lepton spin asymmetry $P_l(q^2)$, the convexity parameter $C_F^l(q^2)$ and other interesting observables.

The remainder of this paper is structured as follows: In Sect. 2, we remind the reader of the theoretical framework of our calculation, including the corresponding low-energy effective Hamiltonian, the form factors, and the helicity amplitudes. We further define various observables expressed in terms of q^2 and NP coupling parameters for the $\Upsilon(nS) \to B_c l \bar{\nu}_l$ decays in this section. The numerical results and discussions about the predictions of observables within the SM and various NP scenarios are presented in Sect. 3. The summary of our work is in Sect. 4.

2 Theory framework

2.1 Effective weak Lagrangian

Assuming the NP scale is higher than the electroweak scale, one can integrate out the possible NP particles as well as the SM heavy particles such as the Z^0, $W^{\pm}$, the top quark and the Higgs boson. To account for both the SM and the effect of

NP, the quark level $b \to c l^- \bar{\nu}_l (l = \tau, \mu, e)$ transition occur through W-exchange and could be described by the effective Lagrangian at $\mu = \mathcal{O}(m_b)$ in a model-independent scheme [72,73]

$$\begin{aligned}\mathcal{L}_{\rm eff} = -\frac{4G_F}{\sqrt{2}} V_{cb} \Big\{ & (1+V_L)\, \bar{l}_L\, \gamma_\mu\, \nu_L\, \bar{q}_L\, \gamma^\mu\, b_L \\ & + V_R\, \bar{l}_L\, \gamma_\mu\, \nu_L\, \bar{q}_R\, \gamma^\mu\, b_R \; + S_L\, \bar{l}_R\, \nu_L\, \bar{q}_R\, b_L \\ & + S_R\, \bar{l}_R\, \nu_L\, \bar{q}_L\, b_R + T_L\, \bar{l}_R\, \sigma_{\mu\nu}\, \nu_L\, \bar{q}_R\, \sigma^{\mu\nu}\, b_L \Big\} + \text{h.c.}, \end{aligned} \tag{1}$$

where G_F is the Fermi constant, V_{cb} denotes the CKM matrix elements and $P_{L,R} = (1 \mp \gamma_5)/2$ as the projection operators. In this work we only consider the NP coupling parameters $V_{L,R}$ and $S_{L,R}$ which characterizing the NP contributions coming from the new vector and scalar interactions. And we also do not consider the contributions of the right-handed neutrinos and the tensor operator. After setting all of the NP couplings to zero, $V_L = V_R = S_L = S_R = 0$, the SM contribution can be obtained obviously. In addition, we also assume that NP effects appear in the tau mode only. And in this section, we list directly the helicity amplitudes and angular distribution which are shown in following text.

Using the Eq. (1), the transition amplitudes can be written as the production of the hadronic matrix element and the leptonic current for the $\Upsilon(nS) \to B_c l^- \bar{\nu}_l$

$$\begin{aligned} & M_{\Upsilon(nS)\to B_c l^-\bar{\nu}_l} \\ & = \frac{G_F}{\sqrt{2}} V_{cb} \sum_k C_k(\mu) \langle B_c|\bar{c}\Gamma^k b|\Upsilon(nS)\rangle\; \bar{u}_\ell\; \Gamma_k\; \nu_\nu, \end{aligned} \tag{2}$$

where Γ^k is the product of gamma matrices that gives rise to various Lorentz structure of leptonic and hadronic currents of Eq. (1). Γ^k is written as $\Gamma^k = \gamma^\mu(1 \pm \gamma_5)$ and $(1 \pm \gamma_5)$. And the $C_k(\mu)$ represents the Wilson coefficient with the values

$$C_k(\mu) = \begin{cases} 1 & \text{for SM} \\ V_{L,R},\, S_{L,R} & \text{for NP} \end{cases}. \tag{3}$$

And the square amplitude can be expressed as the product of leptonic ($L_{\mu\nu}$) and hadronic ($H_{\mu\nu}$) tensor

$$|M_{\Upsilon(nS)\to B_c l\bar{\nu}_l}|^2 = \frac{G_F^2}{2} |V_{cb}|^2 \sum_{ij} C_{i,j}(\mu)(L^{ij}_{\mu\nu} H^{\mu\nu,ij}) \tag{4}$$

and $C_{ij}(\mu)$ denotes the product of Wilson coefficients C_i and C_j. $L_{\mu\nu}$ and $H_{\mu\nu}$ are built from the respective product of the lepton and hadron currents. For convenience, hadronic helicity amplitudes and leptonic helicity amplitudes are generally calculated in the rest frame of $\Upsilon(nS)$ mesons and the $l - \bar{\nu}_l$ center of mass frame, respectively.

2.2 Form factors and helicity amplitudes

Before calculating the hadronic helicity amplitudes, we use the following matrix elements of the vector and axial-vector current for $\Upsilon(nS) \to B_c$ transition

$$\begin{aligned} \langle B_c(p_{B_c})|\bar{c}\gamma_\mu b|\Upsilon(\varepsilon, p_\Upsilon)\rangle &= -\frac{2iV(q^2)}{m_\Upsilon + m_{B_c}} \varepsilon_{\mu\nu\rho\sigma} \varepsilon^\nu p^\rho_{B_c} p^\sigma_\Upsilon\,, \\ \langle B_c(p_{B_c})|\bar{c}\gamma_\mu\gamma_5 b|\Upsilon(\varepsilon, p_\Upsilon)\rangle &= 2m_\Upsilon A_0(q^2)\frac{\varepsilon\cdot q}{q^2} q_\mu \\ & + (m_{B_c} + m_\Upsilon) A_1(q^2)\left(\varepsilon_\mu - \frac{\varepsilon\cdot q}{q^2} q_\mu\right) \\ & + A_2(q^2)\frac{\varepsilon\cdot q}{m_{B_c} + m_\Upsilon}\left[(p_\Upsilon + p_{B_c})_\mu - \frac{m^2_\Upsilon - m^2_{B_c}}{q^2} q_\mu\right], \end{aligned}$$

where $V(q^2)$ and $A_{0,1,2}(q^2)$ are the various QCD form factors for $\Upsilon(nS) \to B_c l\bar{\nu}_l$. And the sign convention in the equation $\varepsilon_{0123} = -1$ and $q \equiv p_\Upsilon - p_{Bc}$.

In the rest frame of the $\Upsilon(nS)$ mesons with a daughter B_c meson moving in the position z direction, more detailed expressions about the momenta and the polarization vectors of the particles $\Upsilon(nS)$, B_c and the virtual W^* can be found in Refs. [10–13].

The matrix elements for the scalar and pseudoscalar currents can also be obtained by using the equation of motion

$$\begin{aligned} i\,\partial_\mu(\bar{c}\gamma^\mu b) &= [m_b - m_c]\bar{c}b \\ i\,\partial_\mu(\bar{c}\gamma^\mu\gamma_5 b) &= -[m_b + m_c]\bar{c}\gamma_5 b \end{aligned}$$

as

$$\begin{aligned} \langle B_c(p_{B_c})|\bar{p}b|\Upsilon(\varepsilon, p_\Upsilon)\rangle &= 0, \\ \langle B_c(p_{B_c})|\bar{p}\gamma_5 b|\Upsilon(\varepsilon, p_\Upsilon)\rangle &= -(\varepsilon\cdot q)\frac{2m_\Upsilon}{m_b + m_c} A_0(q^2), \end{aligned}$$

with the $m_{b,c}$ represent the current quark masses evaluated at the scale $\mu = m_b$. The hadronic parts in the above decomposition are evaluated by using the explicit for matrix elements, the hadronic helicity amplitudes $H^{V_{L,R}}_{\lambda_\Upsilon,\lambda_{W^*}}$ and $H^{S_{L,R}}_{\lambda_\Upsilon,\lambda_{W^*}}$ for the $\Upsilon(nS) \to B_c l\bar{\nu}_l$ are defined as

$$\begin{aligned} H^{V_L}_{\lambda_\Upsilon\lambda_{W^*}}(q^2) &= \bar{\varepsilon}^{*\mu}(\lambda_{W^*})\langle B_c(p_{B_c})|\bar{c}\gamma_\mu(1-\gamma_5)b|\Upsilon(\varepsilon(\lambda_\Upsilon), p_\Upsilon)\rangle, \\ H^{V_R}_{\lambda_\Upsilon\lambda_{W^*}}(q^2) &= \bar{\varepsilon}^{*\mu}(\lambda_{W^*})\langle B_c(p_{B_c})|\bar{c}\gamma_\mu(1+\gamma_5)b|\Upsilon(\varepsilon(\lambda_\Upsilon), p_\Upsilon)\rangle, \\ H^{S_L}_{\lambda_\Upsilon\lambda_{W^*}}(q^2) &= \langle B_c(p_{B_c})|\bar{c}(1-\gamma_5)b|\Upsilon(\varepsilon(\lambda_\Upsilon), p_\Upsilon)\rangle, \\ H^{S_R}_{\lambda_\Upsilon\lambda_{W^*}}(q^2) &= \langle B_c(p_{B_c})|\bar{c}\,(1+\gamma_5)b|\Upsilon(\varepsilon(\lambda_\Upsilon), p_\Upsilon)\rangle, \end{aligned}$$

for simplicity, the notations $\lambda_\Upsilon = 0, \pm$ and $\lambda_{W^*} = 0, \pm, t$ to represent the helicity states of the mesons $\Upsilon(nS)$ and boson W^* will be used in this work.

In a more explicit form, based on the above above hadronic matrix elements with the polarization vectors in the $\Upsilon(nS)$ mesons rest frame, the following non-zero helicity amplitudes in the terms of the various form factors have been

worked out and can be expressed as follows

$$
\begin{aligned}
H_{0t}(q^2) &= H_{0t}^{V_L}(q^2) = -H_{0t}^{V_R}(q^2) = \frac{2m_\Upsilon|\vec{p}|}{\sqrt{q^2}}A_0(q^2),\\
H_{00}(q^2) &= H_{00}^{V_L}(q^2) = -H_{00}^{V_R}(q^2)\\
&= \frac{1}{2m_\Upsilon\sqrt{q^2}}\Big[(m_\Upsilon + m_{B_c})(m_\Upsilon^2\\
&\quad - m_{B_c}^2 + q^2)A_1(q^2) + \frac{4m_\Upsilon^2|\vec{p}|^2}{m_\Upsilon + m_{B_c}}A_2(q^2)\Big],\\
H_{\pm\mp}(q^2) &= H_{\pm\mp}^{V_L}(q^2) = -H_{\mp\pm}^{V_R}(q^2)\\
&= -(m_\Upsilon + m_{B_c})A_1(q^2) \mp \frac{2m_\Upsilon|\vec{p}|}{m_\Upsilon + m_{B_c}}V(q^2),\\
H'_{0t}(q^2) &= H_{0t}^{S_L}(q^2) = -H_{0t}^{S_R}(q^2) = -\frac{2m_\Upsilon|\vec{p}|}{m_b + m_c}A_0(q^2),
\end{aligned}
$$

where $|\vec{p}| = \sqrt{\lambda(m_\Upsilon^2, m_{B_c}^2, q^2)}/(2m_\Upsilon)$ is the momentum of the outgoing meson B_c and the function $\lambda(a,b,c) \equiv a^2 + b^2 + c^2 - 2(ab + bc + ac)$ and q^2 being the momentum transfer squared bounded at $m_l^2 \le q^2 \le (m_\Upsilon - m_{B_c})^2$.

The leptonic helicity amplitudes with the massless right-handed antineutrinos with $\lambda_{\bar{\nu}_l} = 1/2$ can be defined as

$$
\begin{aligned}
h^{V_{L,R}}_{\lambda_l,\lambda_{\bar{\nu}_l}} &= \bar{u}_l(\lambda_l)\gamma^\mu(1 \mp \gamma_5)\nu_{\bar{\nu}}(\lambda_{\bar{\nu}_l})\bar{\varepsilon}_\mu(\lambda_{W^*}),\\
h^{S_{L,R}}_{\lambda_l,\lambda_{\bar{\nu}_l}} &= \bar{u}_l(\lambda_l)(1 \mp \gamma_5)\nu_{\bar{\nu}}(\lambda_{\bar{\nu}_l}),
\end{aligned}
$$

with $\lambda_{W^*} = \lambda_l - \lambda_{\bar{\nu}_l}$. More detail information about the four momenta of lepton and antineutrino pair in the $l - \bar{\nu}_l$ center of mass frame can be found in the Refs. [10,13,74,75]. After taking the exact forms of the spinor and polarization vectors, we obtain following nonvanishing contributions in the $l - \bar{\nu}_l$ center of mass frame

$$
\begin{aligned}
&|h^{V_{L,R}}_{-\frac{1}{2},\frac{1}{2}}|^2 = 8(q^2 - m_l^2), \qquad |h^{V_{L,R}}_{\frac{1}{2},\frac{1}{2}}|^2 = 8\frac{m_l^2}{2q^2}(q^2 - m_l^2),\\
&|h^{S_{L,R}}_{\frac{1}{2},\frac{1}{2}}|^2 = 4(q^2 - m_l^2), \qquad |h^{V_{L,R}}_{\frac{1}{2},\frac{1}{2}}| \times |h^{S_{L,R}}_{\frac{1}{2},\frac{1}{2}}|\\
&= 8\frac{m_l}{2\sqrt{q^2}}(q^2 - m_l^2),
\end{aligned}
$$

and these result exactly have the same expressions as the ones in semileptonic vector B meson decay process [10,13].

2.3 Angular decay distribution of $\Upsilon(nS) \to B_c l^- \bar{\nu}_l$ decays

With all of the above ingredients in hands, we then present the observables considered in our following evaluations. In the presence of NP, the differential angular decay distribution for $\Upsilon(nS) \to B_c l^- \bar{\nu}_l$ decays can be expressed as (both for heavy and light leptons)

$$
\frac{d^2\Gamma}{dq^2 d\cos\theta} = \frac{G_F^2}{192\pi^3}\frac{|\vec{p}|}{m_{B^*}^2}|V_{qb}|^2\left(1 - \frac{m_l^2}{q^2}\right) \times \big|\mathcal{M}(\Upsilon(nS) \to B_c l^- \bar{\nu}_l)\big|^2. \tag{5}
$$

Thus, after including the NP contributions, we can obtain the differential angular distribution for three-body $\Upsilon(nS) \to B_c l^- \bar{\nu}_l$ in terms of q^2, θ_l and helicity amplitudes for a given helicity state ($\lambda_l = \pm\frac{1}{2}$)

$$
\begin{aligned}
&\frac{d^2\Gamma(\lambda_l = -\frac{1}{2})}{dq^2\, d\cos\theta_l}\\
&= \frac{G_F^2|\vec{p}|}{256\pi^3 m_\Upsilon^2}\frac{2}{3}|V_{qb}|^2\, q^2\left(1 - \frac{m_l^2}{q^2}\right)^2\\
&\quad\times\Big\{|1 + V_L|^2\big[(1 - \cos\theta_l)^2 H_{-+}^2\\
&\quad + (1 + \cos\theta_l)^2 H_{+-}^2 + 2\sin^2\theta_l H_{00}^2\big]\\
&\quad + |V_R|^2\big[(1 - \cos\theta_l)^2 H_{+-}^2 + (1 + \cos\theta_l)^2 H_{-+}^2\\
&\quad + 2\sin^2\theta_l H_{00}^2\big] - 4\mathcal{R}e\big[(1 + V_L)V_R^*\big]\\
&\quad\times\big[(1 + \cos\theta_l)^2 H_{+-}H_{-+} + \sin^2\theta_l H_{00}^2\big]\Big\},
\end{aligned} \tag{6}
$$

$$
\begin{aligned}
&\frac{d^2\Gamma(\lambda_l = \frac{1}{2})}{dq^2\, d\cos\theta_l}\\
&= \frac{G_F^2|\vec{p}|}{256\pi^3 m_\Upsilon^2}\frac{2}{3}|V_{qb}|^2\, q^2\left(1 - \frac{m_l^2}{q^2}\right)^2\frac{m_l^2}{q^2}\\
&\quad\times\Big\{\big(|1 + V_L|^2 + |V_R|^2\big)\big[\sin^2\theta_l(H_{-+}^2 + H_{+-}^2)\\
&\quad + 2(H_{0t} - \cos\theta_l H_{00})^2\big] - 4\mathcal{R}e\big[(1 + V_L)V_R^*\big]\\
&\quad\times\big[\sin^2\theta_l H_{-+}H_{+-} + (H_{0t} - \cos\theta_l H_{00})^2\big]\\
&\quad + 4\mathcal{R}e[(1 + V_L - V_R)(S_L^* - S_R^*)]\frac{\sqrt{q^2}}{m_l}\\
&\quad\times\big[H'_{0t}(H_{0t} - \cos\theta_l H_{00})\big] + 2|S_L - S_R|^2\frac{q^2}{m_l^2}{H'_{0t}}^2\Big\},
\end{aligned} \tag{7}
$$

in which, comparing to the B meson semileptonic decays, the decaying of bottom and anti-bottom quarks in $\Upsilon(nS)$ and averaging over the spins of initial state $\Upsilon(nS)$ can causes an additional 2/3. The θ_l is the angle between the directions of the final meson B_c and final lepton l three momentum vector in the dilepton rest frame. From Eq. (7), we find that the distributions for $\lambda_l = -1/2$ do not contain the coupling parameters $S_{L,R}$ which make them totally insensitive to the NP scalar operators.

The normalized differential decay rate depending only on q^2 is then obviously obtained after integrating over the θ_l and summing over the $\lambda_l = 1/2$ and $\lambda_l = -1/2$. The explicit expressions with the NP coupling parameters can be written as

$$\frac{d\Gamma}{dq^2} = \frac{G_F^2|V_{qb}|^2|\vec{p}|}{96\pi^3\, m^2_{\Upsilon(nS)}}\frac{2}{3}\, q^2\left(1-\frac{m_l^2}{q^2}\right)^2 \times\Bigg\{(|1+V_L|^2+|V_R|^2)\Bigg[\left(H^2_{-+}+H^2_{+-}+H^2_{00}\right)\cdot\left(1+\frac{m_l^2}{2q^2}\right)+\frac{3m_l^2}{2q^2}H^2_{0t}\Bigg]-2\mathcal{R}e[(1+V_L)V_R^*]\cdot\Bigg[(2H_{-+}H_{+-}+H^2_{00})\left(1+\frac{m_l^2}{2q^2}\right)+\frac{3m_l^2}{2q^2}H^2_{0t}\Bigg] +3\frac{m_l}{\sqrt{q^2}}\mathcal{R}e\Bigg[(1+V_L-V_R)(S_L^*-S_R^*)\Bigg]H'_{0t}H_{0t} +\frac{3}{2}|S_L-S_R|^2H'^2_{0t}\Bigg\} \tag{8}$$

where the values of the helicity amplitudes are got from Sect. 2.2. If we pick out the H_{00}, H_{0t}, H'_{0t} from Eq. (8), we can get the longitudinal decay rate $d\Gamma^L/dq^2$ of the initial meson $\Upsilon(nS)$. This observable is different from $d\Gamma^L/dq^2$ which is the differential decay width into longitudinally-polarized final meson D^* for the decay process such as $B\to D^* l\bar{\nu}_l$ [76].

There have been a lot of calculations for the differential decay rates of $\Upsilon(nS)\to B_c l^-\bar{\nu}_l$ in the presence of all the operators which are given in Eq. (1). In this paper, we will follow the analytical expressions given in Refs. [12,24,33,77], and consider the other NP sensitive q^2- dependent of the observables which are written as follows:

(i) The differential branching fraction

$$\frac{d\mathscr{B}(\Upsilon(nS)\to B_c l\bar{\nu}_l)}{dq^2} = \tau_{\Upsilon(nS)}\frac{d\Gamma}{dq^2}. \tag{9}$$

(ii) The forward-backward asymmetries parameter for charged lepton

$$A^l_{\rm FB}(q^2) = \left(\int_{-1}^{0} d\cos\theta_l \frac{d^2\Gamma}{dq^2 d\cos\theta_l} - \int_0^1 d\cos\theta_l\frac{d^2\Gamma}{dq^2 d\cos\theta_l}\right)\Big/\frac{d\Gamma}{dq^2}. \tag{10}$$

(iii) The convexity parameter

$$C^l_F(q^2) = \frac{1}{d\Gamma/dq^2}\frac{d^2}{d(\cos\theta_l)^2}\left(\frac{d^2\Gamma}{dq^2 d\cos\theta_l}\right). \tag{11}$$

(iv) The lepton-spin asymmetry:

$$P_l(q^2) = \frac{{\rm d}\Gamma^{\lambda_l=-1/2}/{\rm d}q^2 - {\rm d}\Gamma^{\lambda_l=1/2}/{\rm d}q^2}{{\rm d}\Gamma/{\rm d}q^2}, \tag{12}$$

where ${\rm d}\Gamma^{\lambda_l=\pm1/2}/dq^2$ are differential decay rates for positive and negative helicity of lepton and their detailed expressions can be got after integrating over $\cos\theta_l$ for Eqs. (6) and (7) respectively.

(v) The lepton non-universality observable

$$\mathrm{R}^{(L)}_{B_c}(q^2) = \frac{d\Gamma^{(L)}(\Upsilon(nS)\to B_c\tau\bar{\nu}_\tau)/dq^2}{d\Gamma^{(L)}(\Upsilon(nS)\to B_c\ell\bar{\nu}_\ell)/dq^2}, \tag{13}$$

in which, on the theoretical side, we define

$$d\Gamma(\Upsilon(nS)\to B_c\ell\bar{\nu}_\ell)/dq^2 = \frac{1}{2}\Big[d\Gamma(\Upsilon(nS)\to B_c\mu\bar{\nu}_\mu)/dq^2 + d\Gamma(\Upsilon(nS)\to B_c e\bar{\nu}_e)/dq^2\Big]$$

(vi) The longitudinal and transverse polarizations fraction of initial meson $\Upsilon(nS)$

$$F_L^\Upsilon(q^2) = \frac{d\Gamma^{\lambda_\Upsilon=0}/dq^2}{d\Gamma/dq^2}, \text{ and } F_T^\Upsilon(q^2) = 1-F_L^\Upsilon(q^2). \tag{14}$$

Before continuing, it is interesting to note that similar to the lepton non-universality observable $\mathrm{R}_{B_c}(q^2)$, we also define and construct the following observables to probe the universality of lepton flavor

- Lepton forward and backward fractions

$$\chi_{1,2}(q^2) = \frac{1}{2}\mathrm{R}_{B_c}(q^2)[1\pm A^l_{\rm FB}(q^2)]. \tag{15}$$

- Lepton spin $1/2$ and $-1/2$ fraction

$$\chi_{3,4}(q^2) = \frac{1}{2}\mathrm{R}_{B_c}(q^2)[1\pm P_l(q^2)]. \tag{16}$$

- Ratios of the longitudinal (transverse) polarization asymmetries parameters of the initial meson

$$\mathrm{R}_{F_L^\Upsilon}(q^2) = \frac{F_L^\Upsilon(\Upsilon(nS)\to B_c\tau^-\bar{\nu}_\tau)(q^2)}{F_L^\Upsilon(\Upsilon(nS)\to B_c\mu^-\bar{\nu}_\mu)(q^2)}, \quad \mathrm{R}_{F_T^\Upsilon}(q^2) = \frac{F_T^\Upsilon(\Upsilon(nS)\to B_c\tau^-\bar{\nu}_\tau)(q^2)}{F_T^\Upsilon(\Upsilon(nS)\to B_c\mu^-\bar{\nu}_\mu)(q^2)}. \tag{17}$$

- Ratios of the lepton-spin asymmetry

$$\mathrm{R}_{P_l}(q^2) = \frac{P_l(\Upsilon(nS)\to B_c\tau^-\bar{\nu}_\tau)(q^2)}{P_l(\Upsilon(nS)\to B_c\mu^-\bar{\nu}_\mu)(q^2)}, \tag{18}$$

Note that, the value of CKM matrix elements is canceled to a large extent, so it has no effect on the calculation of these observables. Moreover for q^2 integration of above observables X(q^2) shown in Eqs. (10)–(17), following Ref. [78], in this work two ways of integration are considered. One common method is also called the "normalized integrated" that these observables $\langle X \rangle$ are got by integrating the numerator and denominator over the same q^2 bins separately before taking the ratio. The other method is the so-called "naively integrated" which is defined

$$\overline{X} = \frac{1}{q^2_{\rm max} - q^2_{\rm min}} \int_{q^2_{\rm min}}^{q^2_{\rm max}} dq^2 X(q^2) \tag{19}$$

3 Numerical results and discussion

In the previous sections, we have defined various observables about asymmetries of the spins and angles that can be extracted from the fully differential distribution of the visible final-state kinematics in the $\Upsilon(nS) \to B_c l \bar{\nu}_l$ processes. In order to get a general discussion and ideas about the sensitivities of the above various observables to the different Wilson coefficients C_k listed in Eq. (3), in this section we will select a variety of best fit results inferred from the $\bar{B} \to D^{(*)} \tau^- \bar{\nu}_\tau$ decay resolutions as the NP benchmark points. We will then study how these observables are affected by the various NP scenarios. In this section, we will present our numerical predictions and results for the aforementioned observables of $\Upsilon(nS) \to B_c l \bar{\nu}_l$ both within the SM and in various NP benchmark points in a model independent way. Then we will examine whether the NP effects are large enough to cause siginificant deviations from the SM predictions.

3.1 Input parameters

The main stumbling point in the discussion of the weak interaction processes of hadrons is the theoretical treatment of hadronic form factors. For other input parameters relevant for our numerical computation, such as the masses of various particles and the well-known Fermi coupling constant G_F, we will take the values of these input parameters from the Particle Data Group [39]. For the CKM element, $|V_{cb}| = (41.5 \pm 0.5) \times 10^{-3}$ is fitted by CKMFitter Group in this work [79]. Besides, when we evaluate the branching fractions of the $\Upsilon(nS) \to B_c l \bar{\nu}_l$ decays, the total widths of $\Upsilon(nS)$ mesons are also very important and indispensable. In this work, $\Gamma_{tot}^{\Upsilon(1S,2S,3S)} = (54.02 \pm 1.25,\ 31.98 \pm 2.63,\ 20.32 \pm 1.85)$ keV, and it is very clear to find that $\Gamma_{tot}^{\Upsilon(1S)} > \Gamma_{tot}^{\Upsilon(2S)} > \Gamma_{tot}^{\Upsilon(3S)}$.

In addition, it is important that the form factors about $\Upsilon(nS) \to B_c$ processes defined in Sect. 2.2 are indispensable input parameters especially when calculate the branching fraction. They are calculated and discussed in Refs. [12,59,80,81] within the Bauer Stech Wirbel (BSW) model. And the results evaluated in the BSW model will be used in our work and the dependence of the form factors on q^2 can be explicitly written as

Table 1 The input parameters of the form factors of $\Upsilon(nS) \to B_c$ transition used in this work

Transition	$A_0(0)$	$A_1(0)$	$A_2(0)$	$V(0)$
$\Upsilon(1S) \to B_c$	0.67	0.70	0.51	1.66
$\Upsilon(2S) \to B_c$	0.65	0.69	0.48	1.44
$\Upsilon(3S) \to B_c$	0.57	0.64	0.29	1.25

$$\begin{aligned}
A_0^{\Upsilon(nS)\to B_c}(q^2) &\simeq \frac{A_0(0)}{1 - q^2/m^2_{B_c(0^-)}}, \\
A_1^{\Upsilon(nS)\to B_c}(q^2) &\simeq \frac{A_1(0)}{1 - q^2/m^2_{B_c(1^+)}}, \\
A_2^{\Upsilon(nS)\to B_c}(q^2) &\simeq \frac{A_2(0)}{1 - q^2/m^2_{B_c(1^+)}}, \\
V^{\Upsilon(nS)\to B_c}(q^2) &\simeq \frac{V(0)}{1 - q^2/m^2_{B_c(1^-)}},
\end{aligned} \tag{20}$$

where $m_{B_c}(0^\pm)$ and $m_{B_c}(1^\pm)$ are the pole masses of the states of B_c with quantum number of J^P (J and P are the quantum number of total angular momenta and parity, respectively). More details on the form factors on the values of these masses can easily be found in Table of Ref. [80].

The values at zero-momentum transfer are calculated in Refs. [12] and they are listed in the Table 1.

Similar to the analysis methods used in many work of analogous processes, such $B \to D^{(*)}$, $B^* \to P(V)$, $J/\psi \to P(V)$ and $\Upsilon \to P(V)$ decays, the analysis of form factors and their uncertainties often involves techniques such as linear regression to understand potential sources of error in the input parameters [70,71,82–85].

At the same time, high-luminosity collider experiments are crucial for precisely measuring particle decay processes. The related physical experiments require higher luminosity and precision for the measurement of this particle. However, the accuracy of theoretical calculations may not be able to reach the required precision of experiments in the short term. So, in the subsequent sections about the impact of the NP on aforementioned various observables, to be conservative, 10% uncertainties of the hadronic form factors at $q^2 = 0$ listed in Table 1 will be assigned due to the possible corrections from the high-twist effects and relativistic contributions. In addition, when calculating the theoretical errors of the decay branching ratios and their longitudinal components, 10% the uncertainties of the total width $\Gamma_{\rm tot}^{\Upsilon(nS)}$ and CKM matrix elements V_{cb} are also considered.

The model independent analyses of the NP effects in $b \to c\tau^-\bar{\nu}_\tau$ processes have been done in many previous works. A global fit on the Wilson coefficients of the effective low energy Hamiltonian has been made, and the solutions have also been interpreted in terms of hypothetical NP mediators [9,10,22,76,77,86–93]. In order to illustrate the NP effects on a series of angular distributions in $\Upsilon(nS) \to B_c\tau^-\bar{\nu}_\tau$ decays, we will choose the best-fit values of Wilson coefficients from resent global analyses in Refs. [9,10,87] as our NP benchmark points(BMP). These literatures have taken into account the experimental result on $R(D^{(*)})$, $R(J/\psi)$ and the longitudinal polarization fractions $P_\tau(D^*)$ and $F_L^{D^*}$ reported by BaBar, Belle and LHCb. In order to study in detail the NP effects of various types of Wilson coefficients on individual observables, the Wilson coefficients are classified into three types as follows:

- Case A: we adopt the strategy of switching on one real NP Wilson coefficient V_L, V_R, S_L and S_R at one time. The values are as follows: V_L = -2.07, V_R = -0.0434, S_L = -1.51 and S_R = -1.443. We mark them as BMP1, BMP2, BMP3 and BMP4, respectively.
- Case B: we adopt the strategy of switching on one complex NP Wilson coefficient V_L, V_R, S_L and S_R at one time. The values are as follows: (Re[V_L], Im[V_L]) = $(-1.233, 1.045)$, (Re[V_R], Im[V_R]) = $(-0.030, 0.46)$, (Re[S_L], Im[S_L]) =$(-0.06, 0.31)$ and (Re[S_R], Im[S_R]) = $(-1.35, 0.74)$. We mark them as BMP5, BMP6, BMP7 and BMP8, respectively.
- Case C: we adopt the strategy of switching on two real Wilson coefficients at one time, and the values are as follows: (V_L, V_R) = (0.0694, −0.0026), (V_L, S_L) = (0.0714, −0.0063), (V_L, S_R) = (0.0724, −0.0086), (V_R, S_L) = $(-0.09, 0.1726)$, (V_R, S_R) = $(-0.072, 0.154)$, and (S_L, S_R) = (−1.04, −0.449). We mark them as BMP9-BMP14.

Though the available precise experimental measurements about $\Upsilon(nS) \to B_c l\bar{\nu}_l$ have not yet been measured, the Wilson coefficients appeared in the $b \to c l\bar{\nu}_l$ transitions, especially those relevant to B meson semileptonic decay processes, have already been comprehensively studied in many works. For simplicity, only the central values of best-fit results of the Wilson coefficients are considered as the benchmark point to qualitatively discuss the impact of the NP effect on various physical observables.

3.2 SM prediction for $\Upsilon(nS) \to B_c l\bar{\nu}_l$

Using the transition form factors, the SM theoretical predictions of above various observables with two ways of integration for $\Upsilon(nS) \to B_c l\bar{\nu}_l$ decays undergoing $b \to c l\nu_l$ quark level transitions where l is either lighter leptons (e or μ) or heavier τ lepton have been computed.

These expectation predictions values of many observables are very accurate. Due to the limitation of page space, we present the theoretical results (including errors) of various observables in the SM for the three decay processes in Table 2, respectively. Many of the observables in these processes are being effectively calculated for the first time. These calculations provide an important theoretical foundation for understanding these decay processes and help to test the correctness of the SM as well as explore NP effects.

From the table, we notice that the results for lighter leptons (e or μ) mode is close for $\Upsilon(nS) \to B_c l\bar{\nu}_l$ when $n = 1, 2, 3$ respectively, with two ways of integration. There are three theoretical error for the the branching fractions and its longitudinal component and these errors are mainly caused by the uncertainties of form factor at $q^2 = 0$, total decay widths $\Gamma_{tot}^{\Upsilon(nS)}$ and CKM element V_{cb}, respectively. It is obvious that the theoretical theoretical error are dominated by the input parameters of form factor at $q^2 = 0$ listed in Table 1. For other observables, since they are all in the form of ratios, the uncertainties in the CKM matrix elements and decay widths do not have any impact on these observables. Although only the uncertainties in the form factor contribute to the theoretical errors of the observables in the form of ratios, it can be observed from the table that the errors that introduce to these observables are not particularly significant.

The central value predictsabout about branching fractions and their longitudinal component (in units of 10^{-10}) for $\Upsilon(nS) \to B_c l\bar{\nu}_l$ to be smaller for the τ lepton compared to the lighter leptons (e and μ). It is noteworthy that a clear hierarchical relation $\mathcal{B}^{(L)}(\Upsilon(1S) \to B_c l\bar{\nu}_l) < \mathcal{B}^{(L)}(\Upsilon(2S) \to B_c l\bar{\nu}_l) < \mathcal{B}^{(L)}(\Upsilon(3S) \to B_c l\bar{\nu}_l)$. The reasons that lead to this phenomenon mainly come from two aspects: (i) the relationship on the total decay width of these mesons $\Gamma_{tot}^{\Upsilon(1S)} > \Gamma_{tot}^{\Upsilon(2S)} > \Gamma_{tot}^{\Upsilon(3S)}$; (ii) the relationship on the mass of these mesons $m_{\Upsilon(1S)} < m_{\Upsilon(2S)} < m_{\Upsilon(3S)}$, can also lead to the phase spaces of final states increase with the radial quantum number n. Similar to results on the branching fractions, the same phenomenon of relations for heavier lepton τ mode and lighter leptons (e or μ) modes also appears in the lepton-side asymmetry P_l, longitudinal polarization fraction of initial meson F_L^Υ, χ_2 and χ_3 with two ways of integration. The phenomenon of the central result for heavier lepton τ mode ibeing larger than that for lighter leptons (e of μ) modes appears in A_{FB}, C_F^l, χ_1 and χ_4 with two ways of integration in these three decay processes. Besides, the central results of $C_F^{\mu(e)}$, both P_l and χ_4 only for τ mode, $\chi_{1,2,3}$, $R_{B_c}^{(L)}$ and R_{P_l} increase sequentially for $\Upsilon(nS) \to B_c l\bar{\nu}_l$ decays when $n = 1, 2, 3$, respectively with two ways of integration. In contrast, the central results of C_F^τ and F_L^Υ for μ and e modes decrease sequentially in the semileptonic decays of

$\Upsilon(nS)(n = 1, 2, 3)$, respectively with two ways of integration. The forward–backward asymmetry A^l_{FB} and ratios of the longitudinal polarization asymmetries parameters $R_{F^\Upsilon_L}$ are most peculiar. $\langle A^{\mu(e)}_{FB}\rangle$ and $\langle R_{F^\Upsilon_L}\rangle$ increase sequentially in the semileptonic decays of $\Upsilon(nS)(n = 1, 2, 3)$ with the normalized integrated way. And $\overline{A^\tau_{FB}}$ and $\overline{R_{F^\Upsilon_L}}$ decrease sequentially in the semileptonic decays of $\Upsilon(nS)(n = 1, 2, 3)$ with the naively integrated way. At the same time, all the results of C^l_F and A^l_{FB} are negative in three decay processes with two ways of integration. Moreover, due to all the results of the P_l for e mode are 1, which lead to all the results about χ_4 for e mode are 0 and this is easy to get from Eq. (16).

For the decay branching fraction $\mathcal{B}$, forward backward asymmetry A_{FB}, lepton spin asymmetry P_l and the lepton nonuniversality R_{B_c} by normalized integration, it is observed that our results of these observables of $\Upsilon(1S) \to B_c l\bar{\nu}_l$ decay process are consistent with calculated results in the Refs. [12,70,71,82]. This agreement is also expected, as our form factors also match well. Moreover, relevant research about other different observables have not been studied in the literature so far. At the same time, some of these observables are yet to be identified experimentally. With the continuous improvement and enhancement of high-energy physics experimental conditions, the future can provide important experimental information for the research of $\Upsilon(1S)$, and offer more possibilities for precise $\Upsilon(1S)$ measurements.

To better understand these observables, it is useful to study their q^2 behavior. To simplify, we only depict the dependence of the central values of various observables on q^2, without considering the impact of uncertainties in the input parameters such as form factors, V_{cb} and $\Gamma^{\Upsilon(nS)}_{tot}$. And the impact of unvertainties for these input parameters have been listed in Table 2. Within the reasonable kinematic range, the dependence of the decay width and the various observables introduced above on q^2 are shown in Figs. 1, 2 and 3. The familiar observables such as $d\Gamma/dq^2$, $A^l_{FB}(q^2)$ and $P_l(q^2)$ were also presented for $\Upsilon(nS) \to B_c$ in Ref. [12]. The rest of the observables are shown in this work for the very first time for the SM in Figs. 1, 2 and 3, and for some extensions of the SM in the following figures. It's worth noting that the variation trend of these observables for three decay processes are similar to each other. In these figures, in order to better distinguish the variation tendency of each observable for the final state being different three generations leptons, the red (dot dash), blue (solid) and green (solid) lines indicate the e, μ and τ mode, respectively. It can be clearly observed that for lighter leptons lighter leptons (μ/e mode) compared to heavier epton (τ mode), the dependence of all the observables on q^2 is distinctly differentiated. However, it is difficult to distinct the distribution tendency of $d\Gamma/dq^2$, $A^l_{FB}(q^2)$, $C^l_F(q^2)$, $P_l(q^2)$ and $\chi_4(q^2)$ for lighter leptons (μ, e modes) except in low q^2 region. Furthermore, for the same initial states, the values of $A_{FB}(q^2)$, $C^l_F(q^2)$ and $F^\Upsilon_L(q^2)$ for τ mode is larger than those for $e(\mu)$ mode at a settled point of q^2. And the opposite phenomenon appears in $d\Gamma/dq^2$, $F^\Upsilon_L(q^2)$ and $P_l(q^2)$. Note that for μ mode, the $d\Gamma^{(L)}/dq^2$ changes to zero quickly at the largest recoil range $q^2 \to 0$. We can also find that at the largest recoil range $q^2 \to 0$, the values of $d\Gamma^{(L)}/dq^2$ for $\Upsilon(2S) \to B_c e^-\bar{\nu}_e$ and $\Upsilon(3S) \to B_c e^-\bar{\nu}_e$ are both larger than the $d\Gamma^{(L)}/dq^2$ for $\Upsilon(1S) \to B_c e^-\bar{\nu}_e$ which is below 20. For $\Upsilon(1S) \to B_c l^-\bar{\nu}_l$ decay, the $d\Gamma/dq^2$ of the lighter lepton modes is maximum when $q^2 \approx 6.5\text{GeV}^2$, as well as, the $d\Gamma/dq^2$ of the τ mode is maximum when $q^2 \approx 8\text{GeV}^2$ and approaches zero at q^2_{min} and q^2_{max}. The maximum value of $d\Gamma/dq^2$ for $\Upsilon(nS) \to B_c l^-\bar{\nu}_l(n = 2, 3)$ shifts to a higher q^2 region. The $A_{FB}(q^2)$ is negative for e mode in all q^2 region, and at zero recoil region $q^2 = (m_\Upsilon - m_{B_c})^2$, all the $A_{FB}(q^2)$ is zero. Meanwhile, when $q^2 \to q^2_{\text{min}}$, A^μ_{FB} changes to 0.5 quickly. There are also a SM zero-crossing point for $A^{\mu,\tau}_{FB}$. The SM zero-crossing point of $A^\mu_{FB}(q^2)$ for $\Upsilon(nS) \to B_c\mu^-\bar{\nu}_\mu$ decays are all in small q^2 region with $q^2 \approx 0.5\text{GeV}^2$. The SM zero-crossing point of $A^\tau_{FB}(q^2)$ for $\Upsilon(1S) \to B_c\tau^-\bar{\nu}_\tau$ decay is $q^2 \approx 5.5\text{GeV}^2$ and it shifts to a higer q^2 region for $\Upsilon(nS) \to B_c l^-\bar{\nu}_l(n = 2, 3)$. All the $C^l_F(q^2)$ are negative in the whole q^2 region. $C^{\mu(\tau)}_F = 0$ at q^2_{min} and q^2_{max} for $\Upsilon(nS) \to B_c l^-\bar{\nu}_l(n = 1, 2, 3)$. In the small q^2 region $C^e_F = -1.5$ at q^2_{min}, and $C^\mu_F = -1.25$ when $q^2 \approx 0.4\text{GeV}^2$ and it changes to zero quickly when $q^2 \to q^2_{\text{min}}$. Furthermore, the $C^{\mu(e)}_F(q^2)$ great increasing with the q^2 except in the small q^2 region. The $C^\tau_F(q^2)$ is small in the whole q^2 range, which implies a straight line behavior of the $\cos\theta$ distribution.

From Fig. 1, one can also see that the variation trends of longitudinal and transverse polarization fraction of initial meson $F^\Upsilon_L(q^2)$ and $F^\Upsilon_T(q^2)$, present an axial symmetric distribution in the horizontal direction between each other. And the corresponding axis of symmetry is the horizontal line where the vertical axis values is 0.5. All the $F^\Upsilon_L(q^2)$ are great decreasing with q^2 over the whole q^2 region, so the opposite phenomenon (increase phenomenon) appears in $F^\Upsilon_T(q^2)$ and this is easy to get from Eq. (14). Note that for the lighter lepton modes, at q^2_{min} the F^Υ_L is 1. However, for τ mode, at $q^2_{\text{min}} = m^2_\tau$, $F^{\Upsilon(1S)}_L \to 0.69$ and $F^{\Upsilon(2S,3S)}_L \to 0.75$. We have observed the feature of F^Υ_L and F^Υ_T that the e mode and μ mode overlap completely over the entire q^2 region. For the lepton spin asymmetry $P_l(q^2)$, it is clear to find that all the P_e is +1 in the whole q^2 ranges and P_μ changes to -0.3 quickly when $q^2 \to q^2_{\text{min}}$. For the heavier lepton mode, $P_\tau(q^2)$ is great increasing with q^2 in the whole q^2 region and there is a SM zero-crossing point at $q^2 \approx 3.3\text{GeV}^2$ for $\Upsilon(1S) \to B_c\tau^-\bar{\nu}_\tau$ and $q^2 \approx 3.5\text{GeV}^2$ for $\Upsilon(2S, 3S) \to B_c\tau^-\bar{\nu}_\tau$.

As can be seen from the Fig. 2, which represents the trend of the observables listed in Eqs. (15) and (16). For

Table 2 The SM values for the branching fractions $\mathcal{B}^{(L)}$, the forward backward asymmetry A^l_{FB}, the convexity factor C^l_F, the lepton-spin asymmetry P_l, the longitudinal polarization fraction of initial meson $P_L^{\Upsilon(nS)}$, four observables $\chi_{1,2,3,4}$ and the lepton non-universality $\mathrm{R}^{(L)}_{B_c}$ for the e mode, μ mode and τ mode with two ways of integration for $\Upsilon(nS) \to B_c l \bar{\nu}_l$ channel

	$\Upsilon(1S) \to B_c l\nu$			$\Upsilon(2S) \to B_c l\nu$			$\Upsilon(3S) \to B_c l\nu$		
	τ mode	μ mode	e mode	τ mode	μ mode	e mode	τ mode	μ mode	e mode
$\mathcal{B}(10^{-10})$	$1.262^{+0.237+0.030+0.081}_{-0.215+0.029+0.079}$	$5.372^{+1.036+0.127+0.345}_{-0.941-0.121-0.334}$	$5.397^{+1.045+0.128+0.347}_{-0.949-0.122-0.336}$	$7.826^{+1.263+0.701+0.503}_{-1.160-0.595-0.487}$	$20.569^{+3.433+1.184+1.322}_{-3.157-1.563-1.281}$	$20.636^{+3.454+1.849+1.326}_{-3.176-1.568-1.285}$	$19.914^{+3.511+1.995+1.280}_{-3.200-1.662-1.240}$	$43.186^{+7.895+4.326+2.775}_{-7.204-3.604-2.689}$	$43.299^{+7.932+4.337+2.782}_{-7.238-3.613-2.696}$
$\mathcal{B}^{\mathrm{L}}(10^{-10})$	$0.542^{+0.095+0.013+0.035}_{-0.086-0.012-0.034}$	$2.682^{+0.519+0.064+0.172}_{-0.473-0.061-0.167}$	$2.697^{+0.526+0.064+0.173}_{-0.480-0.061-0.168}$	$3.433^{+0.521+0.308+0.221}_{-0.479-0.261-0.214}$	$10.037^{+1.680+0.899+0.645}_{-1.550-0.763-0.625}$	$10.075^{+1.565+0.903+0.647}_{-1.696-0.766-0.627}$	$8.586^{+1.438+0.860+0.552}_{-1.313-0.716-0.535}$	$20.225^{+3.752+2.026+1.300}_{-3.432-1.688-1.259}$	$20.286^{+3.780+2.032+1.304}_{-3.458-1.693-1.263}$
$\langle A^l_{FB} \rangle$	$-0.069^{+0.050}_{-0.050}$	$-0.357^{+0.075}_{-0.090}$	$-0.360^{+0.077}_{-0.092}$	$-0.105^{+0.031}_{-0.033}$	$-0.248^{+0.049}_{-0.056}$	$-0.250^{+0.049}_{-0.057}$	$-0.086^{+0.025}_{-0.035}$	$-0.206^{+0.024}_{-0.025}$	$-0.208^{+0.024}_{-0.026}$
$\overline{A^l_{FB}}$	$-0.004^{+0.019}_{-0.019}$	$-0.179^{+0.023}_{-0.024}$	$-0.187^{+0.023}_{-0.024}$	$-0.018^{+0.187}_{-0.190}$	$-0.183^{+0.021}_{-0.022}$	$-0.189^{+0.021}_{-0.022}$	$-0.036^{+0.019}_{-0.019}$	$-0.190^{+0.022}_{-0.023}$	$-0.195^{+0.023}_{-0.024}$
$\langle C^l_F \rangle$	$-0.047^{+0.003}_{-0.003}$	$-0.361^{+0.013}_{-0.012}$	$-0.374^{+0.013}_{-0.012}$	$-0.069^{+0.004}_{-0.004}$	$-0.339^{+0.012}_{-0.011}$	$-0.349^{+0.012}_{-0.011}$	$-0.072^{+0.005}_{-0.004}$	$-0.297^{+0.011}_{-0.010}$	$-0.304^{+0.011}_{-0.010}$
$\overline{C^l_F}$	$-0.045^{+0.003}_{-0.003}$	$-0.395^{+0.013}_{-0.012}$	$-0.414^{+0.012}_{-0.011}$	$-0.069^{+0.005}_{-0.004}$	$-0.394^{+0.012}_{-0.011}$	$-0.408^{+0.012}_{-0.011}$	$-0.075^{+0.006}_{-0.005}$	$-0.371^{+0.012}_{-0.011}$	$-0.383^{+0.012}_{-0.010}$
$\langle P_l \rangle$	$0.537^{+0.023}_{-0.027}$	$0.987^{+0.002}_{-0.002}$	1	$0.602^{+0.023}_{-0.026}$	$0.991^{+0.001}_{-0.002}$	1	$0.645^{+0.021}_{-0.025}$	$0.993^{+0.001}_{-0.001}$	1
$\overline{P_l}$	$0.450^{+0.029}_{-0.033}$	$0.980^{+0.003}_{-0.003}$	1	$0.505^{+0.029}_{-0.032}$	$0.985^{+0.002}_{-0.002}$	1	$0.542^{+0.014}_{-0.015}$	$0.987^{+0.002}_{-0.002}$	1
$\langle F_L^{\Upsilon(nS)} \rangle$	$0.429^{+0.010}_{-0.009}$	$0.499^{+0.005}_{-0.006}$	$0.499^{+0.005}_{-0.006}$	$0.439^{+0.009}_{-0.008}$	$0.488^{+0.005}_{-0.005}$	$0.488^{+0.005}_{-0.005}$	$0.431^{+0.008}_{-0.007}$	$0.468^{+0.004}_{-0.005}$	$0.468^{+0.004}_{-0.005}$
$\overline{F_L^{\Upsilon(nS)}}$	$0.469^{+0.011}_{-0.010}$	$0.518^{+0.005}_{-0.005}$	$0.518^{+0.005}_{-0.006}$	$0.484^{+0.010}_{-0.009}$	$0.515^{+0.005}_{-0.005}$	$0.515^{+0.005}_{-0.005}$	$0.480^{+0.010}_{-0.009}$	$0.504^{+0.005}_{-0.005}$	$0.504^{+0.005}_{-0.005}$
$\langle \chi_1 \rangle$	$0.109^{+0.006}_{-0.006}$	$0.076^{+0.009}_{-0.010}$	$0.075^{+0.009}_{-0.010}$	$0.170^{+0.006}_{-0.006}$	$0.142^{+0.009}_{-0.010}$	$0.142^{+0.009}_{-0.010}$	$0.211^{+0.006}_{-0.005}$	$0.182^{+0.005}_{-0.005}$	$0.182^{+0.005}_{-0.005}$
$\overline{\chi_1}$	$0.164^{+0.005}_{-0.004}$	$0.135^{+0.003}_{-0.003}$	$0.134^{+0.003}_{-0.003}$	$0.219^{+0.006}_{-0.006}$	$0.181^{+0.005}_{-0.004}$	$0.181^{+0.005}_{-0.004}$	$0.242^{+0.007}_{-0.006}$	$0.202^{+0.005}_{-0.005}$	$0.202^{+0.005}_{-0.005}$
$\langle \chi_2 \rangle$	$0.126^{+0.006}_{-0.006}$	$0.160^{+0.012}_{-0.010}$	$0.160^{+0.012}_{-0.010}$	$0.210^{+0.008}_{-0.007}$	$0.237^{+0.012}_{-0.011}$	$0.237^{+0.012}_{-0.011}$	$0.250^{+0.005}_{-0.004}$	$0.278^{+0.008}_{-0.007}$	$0.278^{+0.008}_{-0.007}$
$\overline{\chi_2}$	$0.166^{+0.003}_{-0.003}$	$0.195^{+0.006}_{-0.005}$	$0.195^{+0.006}_{-0.005}$	$0.227^{+0.004}_{-0.004}$	$0.264^{+0.008}_{-0.007}$	$0.264^{+0.008}_{-0.007}$	$0.260^{+0.005}_{-0.005}$	$0.300^{+0.009}_{-0.008}$	$0.300^{+0.009}_{-0.008}$
$\langle \chi_3 \rangle$	$0.181^{+0.001}_{-0.002}$	$0.235^{+0.003}_{-0.003}$	$0.235^{+0.003}_{-0.003}$	$0.305^{+0.002}_{-0.002}$	$0.379^{+0.005}_{-0.004}$	$0.380^{+0.005}_{-0.005}$	$0.379^{+0.001}_{-0.002}$	$0.459^{+0.005}_{-0.005}$	$0.461^{+0.006}_{-0.005}$
$\overline{\chi_3}$	$0.239^{+0.002}_{-0.002}$	$0.326^{+0.005}_{-0.004}$	$0.329^{+0.005}_{-0.004}$	$0.336^{+0.002}_{-0.002}$	$0.443^{+0.006}_{-0.005}$	$0.445^{+0.007}_{-0.006}$	$0.387^{+0.002}_{-0.002}$	$0.498^{+0.007}_{-0.006}$	$0.501^{+0.007}_{-0.006}$
$\langle \chi_4 \rangle$	$0.054^{+0.004}_{-0.003}$	$0.001^{+0.0003}_{-0.0002}$	0	$0.076^{+0.006}_{-0.005}$	$0.002^{+0.0003}_{-0.0003}$	0	$0.082^{+0.007}_{-0.006}$	$0.002^{+0.0003}_{-0.0002}$	0
$\overline{\chi_4}$	$0.091^{+0.007}_{-0.006}$	$0.003^{+0.0006}_{-0.0005}$	0	$0.111^{+0.009}_{-0.008}$	$0.003^{+0.0006}_{-0.0005}$	0	$0.115^{+0.010}_{-0.008}$	$0.003^{+0.0005}_{-0.0005}$	0
$\langle \mathrm{R}_{B_c} \rangle$		$0.235^{+0.003}_{-0.003}$			$0.380^{+0.005}_{-0.005}$			$0.461^{+0.006}_{-0.005}$	
$\overline{\mathrm{R}_{B_c}}$		$0.330^{+0.005}_{-0.004}$			$0.447^{+0.007}_{-0.006}$			$0.501^{+0.007}_{-0.006}$	
$\langle \mathrm{R}^L_{B_c} \rangle$		$0.202^{+0.007}_{-0.006}$			$0.342^{+0.011}_{-0.010}$			$0.425^{+0.013}_{-0.011}$	
$\overline{\mathrm{R}^L_{B_c}}$		$0.354^{+0.012}_{-0.010}$			$0.479^{+0.016}_{-0.013}$			$0.535^{+0.017}_{-0.014}$	
$\langle \mathrm{R}_{F_L^\Upsilon} \rangle$		$0.624^{+0.015}_{-0.013}$			$0.729^{+0.015}_{-0.014}$			$0.772^{+0.016}_{-0.014}$	
$\overline{\mathrm{R}_{F_L^\Upsilon}}$		$1.107^{+0.026}_{-0.023}$			$1.097^{+0.022}_{-0.019}$			$1.089^{+0.021}_{-0.018}$	
$\langle \mathrm{R}_{F_T^\Upsilon} \rangle$		$0.760^{+0.015}_{-0.017}$			$0.826^{+0.015}_{-0.016}$			$0.851^{+0.014}_{-0.016}$	
$\overline{\mathrm{R}_{F_T^\Upsilon}}$		$0.907^{+0.019}_{-0.022}$			$0.904^{+0.018}_{-0.020}$			$0.909^{+0.017}_{-0.019}$	
$\langle \mathrm{R}_{P_l} \rangle$		$0.317^{+0.019}_{-0.022}$			$0.398^{+0.022}_{-0.024}$			$0.446^{+0.022}_{-0.024}$	
$\overline{\mathrm{R}_{P_l}}$		$0.451^{+0.029}_{-0.033}$			$0.506^{+0.029}_{-0.032}$			$0.543^{+0.028}_{-0.031}$	

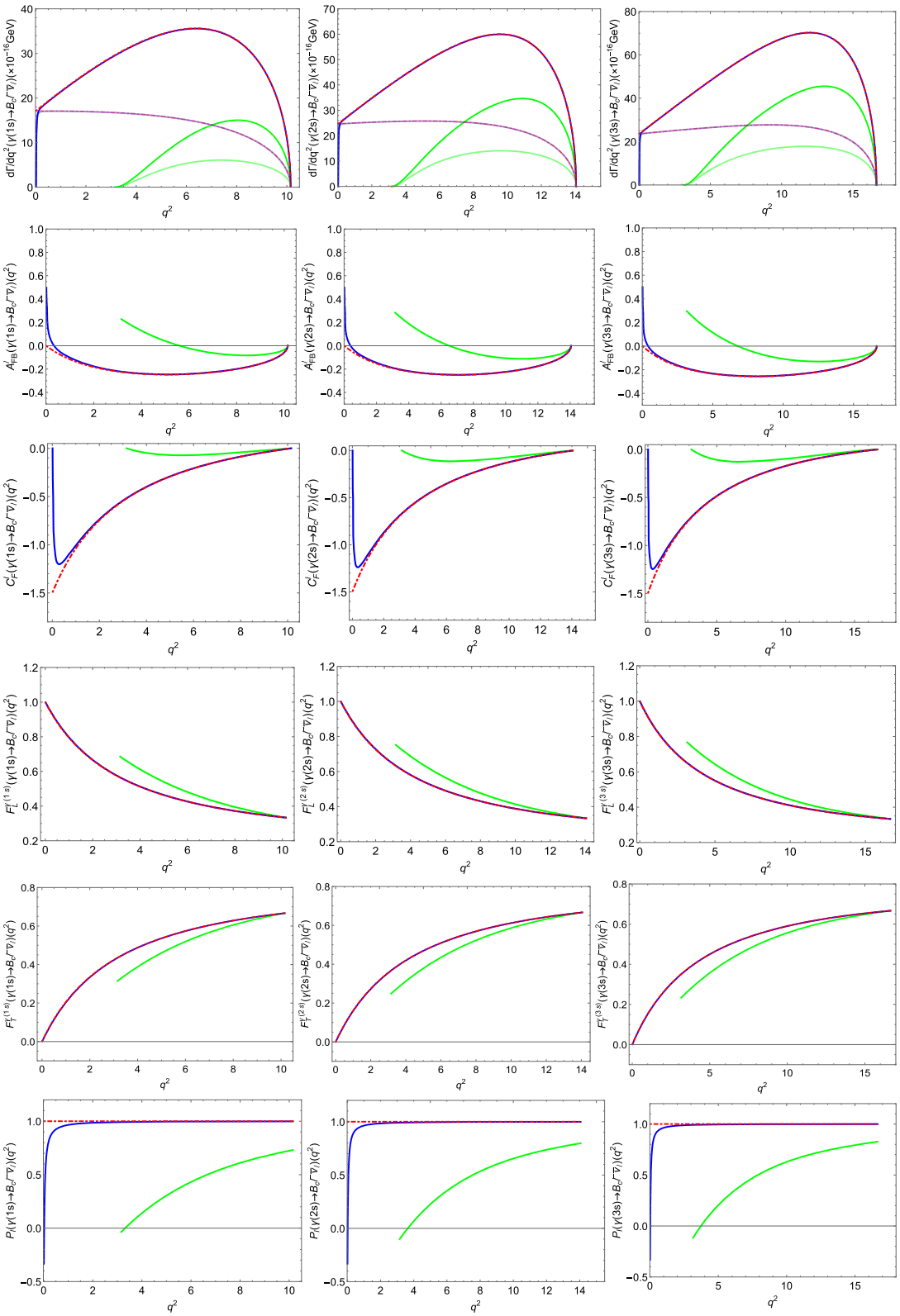

Fig. 1 The q^2 distributions of the observables $d\Gamma/dq^2$,$A^l_{FB}(q^2)$, $C^l_F(q^2)$,$F^{\Upsilon(nS)}_T$,$F^{\Upsilon(nS)}_T$ and $P_l(q^2)$ for the decays $\Upsilon(nS) \to B_c l \bar{\nu}_l$ with n=1 (left column), 2 (middle column), 3 (right column) in the SM. The red (dot dash), blue (solid), and green (solid) lines indicate the e, μ and τ mode, respectively. The corresponding light colours for $d\Gamma/dq^2$ indicate the longitudinal decay rate $d\Gamma^L/dq^2$. And the same in Fig. 2

the τ mode, all of $\chi_{1,2,3}(q^2)$ increase significantly with q^2 throughout the entire q^2 region. However, for lighter lepton modes, $\chi_{1,2,3}(q^2)$ decrease significantly with q^2 when $0 < q^2 < m_\tau^2$ and increase siginificantly with q^2 when $m_\tau^2 < q^2 < q^2_{\rm max}$. One can find that for the same initial states, when $q^2 \to q^2_{\rm max}$, the value of $\chi_{1(2)}(q^2)$ for both lighter lepton modes and τ mode are same. Furthermore, for the same initial states, at a settled point of q^2, the values of $\chi_{1(4)}$ for τ mode are larger than those for $e(\mu)$ mode. Conversely, the opposite phenomenon occurs in $\chi_{2(3)}(q^2)$.

In Fig. 3, we analyze sequentially the q^2 distributions of the ratios of branching fraction $R^{(L)}_{B_c}(q^2)$, and ratios of the longitudinal (transverse) polarization asymmetries parameters of the initial meson $R_{F^\Upsilon_{L(T)}}(q^2)$, as well as, ratios of the lepton-spin asymmetry $R_{P^\Upsilon_l}(q^2)$. It is clear to find that $R^{(L)}_{B_c}(q^2)$, $R_{F^\Upsilon_T}(q^2)$ and $R_{P^\Upsilon_l}(q^2)$ all increase with q^2 over the whole q^2 region. Furthermore, it is very evident from the first picture of Fig. 3, in which the SM prediction of the longitudinal branching fraction ratios $R^L_{B_c}$, displayed by the light colour, is larger than the result of R_{B_c} for the $\Upsilon(nS) \to B_c l \bar{\nu}_l$ processes at a settled point of q^2. At the same time, it is evident that the result of $R^{(L)}_{B_c}$ becomes larger in turn for the decays $\Upsilon(1S) \to B_c l \bar{\nu}_l$, $\Upsilon(2S) \to B_c l \bar{\nu}_l$, and $\Upsilon(3S) \to B_c l \bar{\nu}_l$, respectively, at a settled point of q^2. Conversely, the opposite phenomenon arises in $R_{F^\Upsilon_T}(q^2)$ and $R_{P^\Upsilon_l}(q^2)$. These two observables are also increasing with q^2 over the whole q^2 region. It should also be noted that $R_{F^\Upsilon_T}$ is decreasing with q^2 over the whole q^2 region, and there is also no continuous distribution of size relationships for this observable. Though there is symmetric phenomenon between F^Υ_L and F^Υ_T, it is obvious from the figure that there is no such symmetry between $R_{F^\Upsilon_L}$ and $R_{F^\Upsilon_T}$ at a settled point of q^2.

3.3 New physics effects analysis on $\Upsilon(nS) \to B_c \tau \bar{\nu}_\tau$

Let us now focus on the impact of the vector and scalar NP Wilson coefficients on the above mentioned different physical observables, and examin their discriminatory power for NP in the semileptonic decays of $\Upsilon(nS) \to B_c \tau^- \bar{\nu}_\tau$. As can be seen from to the previous analysis, the variation trends of various observables for the $\Upsilon(nS) \to B_c \tau^- \bar{\nu}_\tau$ processes with $n = 1, 2, 3$ are similar to each other. In order to avoid unnecessary repetition of the description, we will take the $\Upsilon(3S) \to B_c \tau^- \bar{\nu}_\tau$ process as an example for the detailed analysis on the NP effects.

We will broadly analyze all the available information about the NP effects on the above mentioned various observables, following the different NP scenarios presented in Figs. 4 and 5. The q^2 dependency distribution of the observables $d\Gamma/dq^2$, $A^\tau_{FB}(q^2)$, $C^\tau_F(q^2)$, $F^\Upsilon_L(q^2)$, $F^\Upsilon_T(q^2)$ and $P_\tau(q^2)$, for $\Upsilon(3S) \to B_c \tau^- \bar{\nu}_\tau$ decay mode, both in the SM case and including the contribution from different types of NP scenarios, are presented in Fig. 4. In the figure, we distinguish the results for both SM and various NP scenarios using different colors, respectively. The width of each curve is derived from the theoretical uncertainties of the input parameters, which include hadronic form factors. In this work, we temporarily do not take into account the impact of the uncertainties of NP coupling parameters on the errors of various observables. From these figures, we make the following observations:

- After considering the contribution of various real NP coupling parameters in the case A, it is observed that the differential decay rate $d\Gamma/dq^2$ exhibits a more pronounced deviation from the SM prediction when the BMP1, BMP2 and BMP3 scenarios are considered, as opposed to the situation with the BMP4 scenario. There is a significant enhancement effect on $d\Gamma/dq^2$ after considering the contribution of NP for BMP1, BMP2 and BMP3 scenarios. A shared characteristic is observed near the zero recoil point, where the predictions under various NP scenarios align with those of SM for these observables. $A_{FB}(q^2)$ shows a distinct deviation from the prediction of SM across the entire q^2 range for the BMP3 and BMP4 scenarios. In BMP3 scenario, $A_{FB}(q^2)$ is enhanced relative to the scalar coupling, while in the BMP4 scenario, it is decreased throughout the entire q^2 region. Besides, when compared to the zero-crossing point of the SM, the zero-crossing point of $A_{FB}(q^2)$ is observed to shifts to a significant lower q^2 value in the BMP3 scenario due to the scalar coupling. Conversely, in the BMP4 scenario, the zero crossing point of $A_{FB}(q^2)$ moves to a notably higher q^2 values as a result of the scalar coupling. No sizable deviation is observed for $A_{FB}(q^2)$ in the presence of vector coupling in BMP1 scenario. The similar phenomenon is also found in $C^\tau_F(q^2)$ and $F^\Upsilon_L(q^2)$. And the opposite phenomenon that BMP4 caused a significant enhancement effect for lower q^2 region and BMP3 caused a significant decrease effect for entire q^2 region appears in $F^\Upsilon_T(q^2)$ and $P_\tau(q^2)$. In addition, after accounting for the NP contribution of scalar coupling in the BMP4 scenario, $F^\Upsilon_T(q^2)$ and $P_\tau(q^2)$ no longer exhibit zero crossing point. In contrast, zero-crossing points are present in the predictions of the SM as well as in the BMP1,BMP2, and BMP3 scenarios. So measuring these observables in the corresponding q^2 region will further substantiate the observed anomalies in b-decays.
- Though the NP coupling parameters are set to the complex in case B, the NP effects on different observables for these NP scenarios are similar to the prediction results in Case A. The differential decay rate $d\Gamma/dq^2$ is enhanced with respect to the vector coupling but shows no sizable deviation for the scalar coupling over the whole q^2

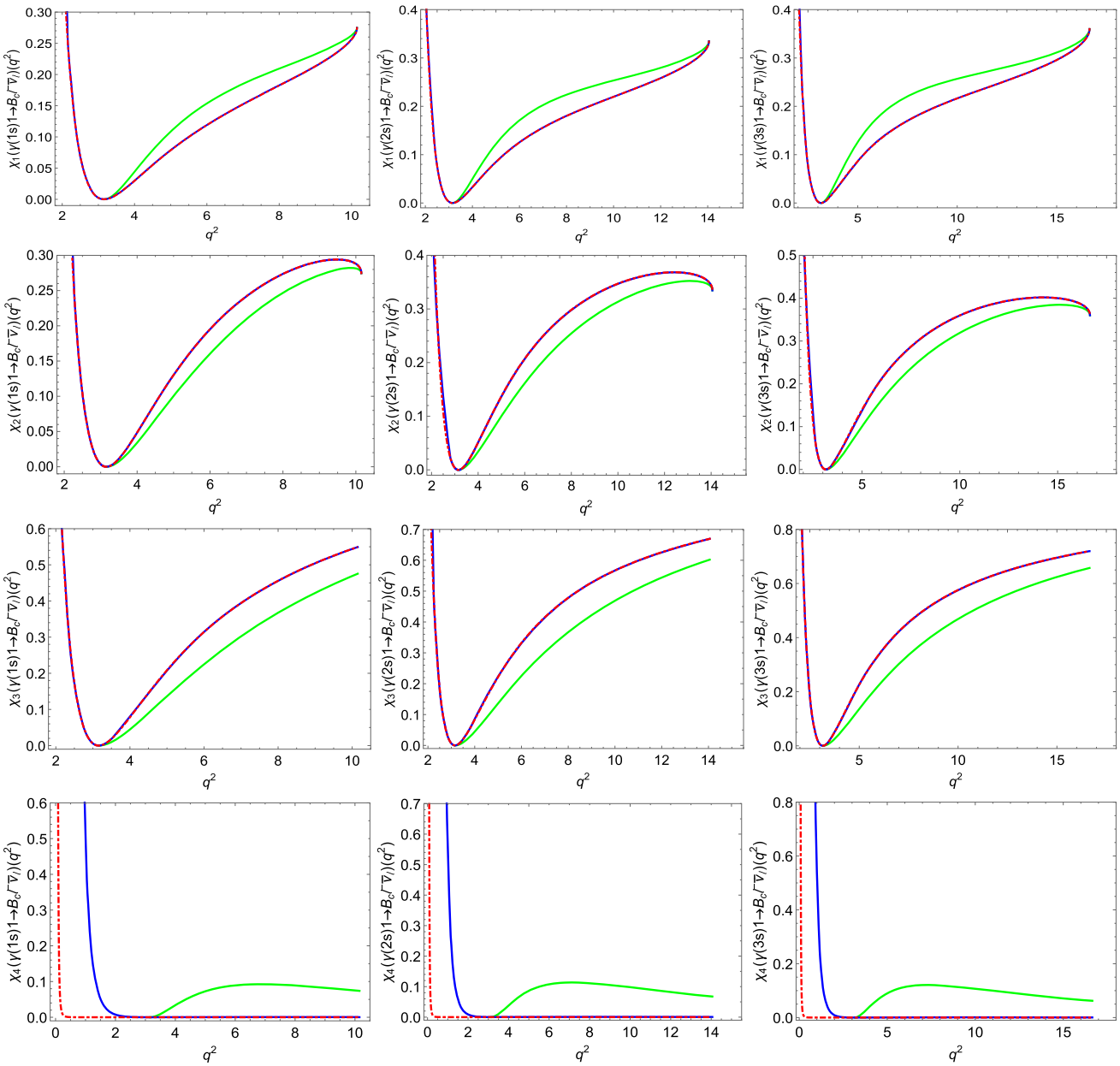

Fig. 2 The q^2 distributions of the observables $\chi_1(q^2)$, $\chi_2(q^2)$,$\chi_3(q^2)$ and $\chi_4(q^2)$ for the decays $\Upsilon(nS) \to B_c l \bar{\nu}_l$ in the SM

region. $A_{FB}^{\tau}(q^2)$ is enhanced compared to the SM prediction for the vector coupling in the BMP6 scenario, but it is significantly decreased in the BMP8 scenario over the whole q^2 region. Additionally, the zero crossing point of $A_{FB}^{\tau}(q^2)$ shifts to a significant lower and higher q^2 value. For $C_F^{\tau}(q^2)$, $F_{L(T)}^{\Upsilon}(q^2)$ and $P_{\tau}(q^2)$, different from the results considering the NP coupling in case A, there is a slight deviation from the SM prediction in the lower q^2 range for these four observables when considering the NP contribution in BMP8 scenario. The measurement of this four observables may do not further endorse existence of NP beyond the SM in this case. However, measuring these observables may provide insight into distinguishing the contribution of the scalar coupling for the S_R parameter from other types of NP coupling contributions.

- From the last column in Fig. 4 in which two real NP coupling parameters are considered at a time in case C. One can see that the q^2 dependence of $d\Gamma/dq^2$ is similar to the case A. In various NP scenarios, except for BMP14 scenario, $d\Gamma/dq^2$ is enhanced compared for the SM prediction. $A_{FB}(q^2)$ displays a distinctive deviation from the prediction of SM in the entire q^2 range for BMP13 and BMP14 scenarios in which S_R parameters is considered. There is a slight deviation from the prediction of

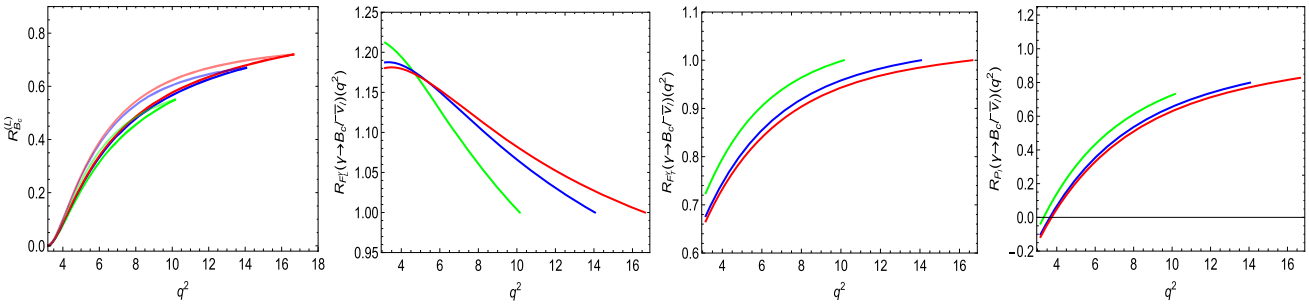

Fig. 3 The q^2 distributions of the observables $R^{(L)}_{B_c}(q^2)$, $R_{F^{\Upsilon}_L}(q^2)$, $R_{F^{\Upsilon}_T}(q^2)$ and $R_{P_l}(q^2)$. The corresponding light colours for R_{B_c} indicate the longitudinal $R^L_{B_c}$. Note that the colors in this figures is a different from Figs. 1 and 2. The green, blue and red solid lines in this figures indicate the $\Upsilon(nS) \to B_c l \bar{\nu}_l (n = 1, 2, 3)$ processes, respectively

SM in the lower q^2 range for $F^{\Upsilon}_{L(T)}(q^2)$ and $P_\tau(q^2)$ when consider the NP contribution for BMP13 and BMP14 scenarios in which S_R parameters is considered.

In order to better and further distinguish these different NP scenarios, we need to continue studying some observables that are similar to the ratio R_{B_c} and they are displayed in Eqs. (15), (16) and (17). And the q^2 dependence of these observables is displayed in Fig. 5. Though the NP effect in NP scenarios which contain S_R coupling parameter contributes the most to $\chi_2(q^2)$, there is no much impact on $\chi_2(q^2)$, even when the uncertainties of the some input parameter have been taken into account for all three cases. The predicted value of $\chi_3(q^2)$ decreases slightly in the BMP3, BMP4, BMP8 and BMP14 scenarios. And the predictions of $\chi_3(q^2)$ in the SM and other NP scenarios have overlapped with each other completely. The same phenomenon also appears in the $R_{B_c}(q^2)$, except for the result of the BMP3 scenario. The BMP4 scenario can significantly decrease the predicted values of $\chi_1(q^2)$, $\chi_4(q^2)$, and $R_{F^{\Upsilon}_L}(q^2)$. But the BMP3 scenario can increase the predicted values of these observables. Furthermore, the BMP8 scenario in Case B and the BMP14 scenario in Case C can also significantly decrease the predicted values of above three observables. The opposite change phenomenon occurs in $R_{F^{\Upsilon}_T}(q^2)$. In addition, there is a zero crossing point for $R_{F^{\Upsilon}_T}(q^2)$ when considering NP contribution of the BMP3 and BMP13 scenarios. In contrast, there are no zero crossing points in the SM and in other NP scenarios. There is also a very obvious feature that when q^2 tends to the endpoint $q^2_{\rm max}$, the prediction of this observable is a fixed value both in SM and in all NP scenarios. And when q^2 tends to the endpoint $q^2_{\rm min}$, the values of $\chi_{1,2,3,4}$ are all zero. The measurement of the above observables may further endorse the existence of NP signals beyond the SM.

4 Summary

The most experimentally observed phenomena have been explained elegantly by SM, and there is no new particle beyond SM have been discovered thus far. However, there are some deviations from SM prediction have been observed in the B hadron decay transitions involving the third generation of lepton, especially in the $b \to c\tau\bar{\nu}_\tau$ process. In this scenario, it is very important to investigate thoroughly how to explain these indirect signals of NP. With the sharp increase in the $\Upsilon(1S)$ data samples at high luminosity dedicated heavy flavor factories, the bottomonium weak decay, especially the weak decay of $\Upsilon(1S)$, is interesting for exploring the underlying mechanism responsible for transition between the heavy quarks, over-constraining parameters from B decay processes, and investigating perturbative or non-perturbative effects. The weak decays of $\Upsilon(1S)$ are also legal in the SM, though their branching ratios are expected to be tiny in comparison to the conventional strong and electromagnetic decays. Motivated by several anomalies $R_{D^{(*)}}$ and $R_{J/\psi}$ observed in semileptonic B meson decays as well as the abundant $\Upsilon(nS)$ data sample at high luminosity heavy flavor experiments in the future, we perform a detail analysis for the semileptonic $\Upsilon(nS) \to B_c l^- \bar{\nu}_l$ which is also induced by the $b \to c\tau\bar{\nu}_\tau$ quark level transition as $B \to D^{(*)}\tau\bar{\nu}_\tau$ processes.

Using the form factors of the transition $\Upsilon(nS) \to B_c$, which are calculated in the Bauer-Stech-Wirbel framework, the SM prediction values of various observables that is in the form of ratios for the decays $\Upsilon(nS) \to B_c l^- \bar{\nu}_l$ are first calculated. Then the contribution of NP parameters mainly come from vector and scalar couplings to different observables relative to $\Upsilon(3S) \to B_c \tau^- \bar{\nu}_\tau$ are also discussed in various NP scenarios. The results show that the many observables after considering the contributions of NP couplings, have significant deviations from the prediction of the SM. No sizable deviation is observed for $d\Gamma/dq^2$ in the presence of scalar

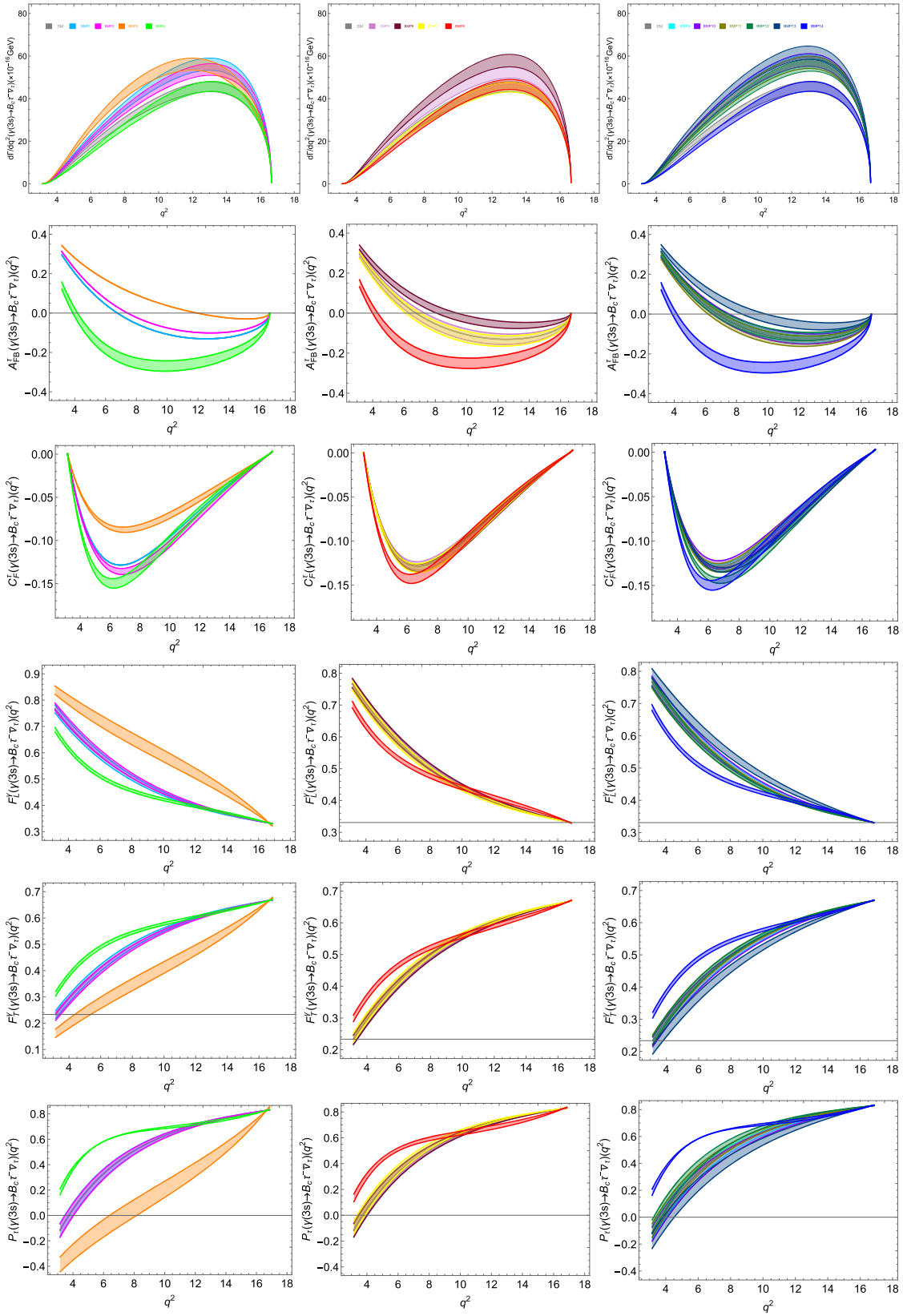

Fig. 4 The q^2 distributions of the various observables for the decays $\Upsilon(3S) \to B_c \tau \bar{\nu}_\tau$ in the SM, case A (left column), case B (middle column), case C (right column) NP scenarios, respectively. Apart from the differential decay rates, the band widths represent the theoretical uncertainties of other observables only comes from hadronic form factors. And the same in Fig. 5

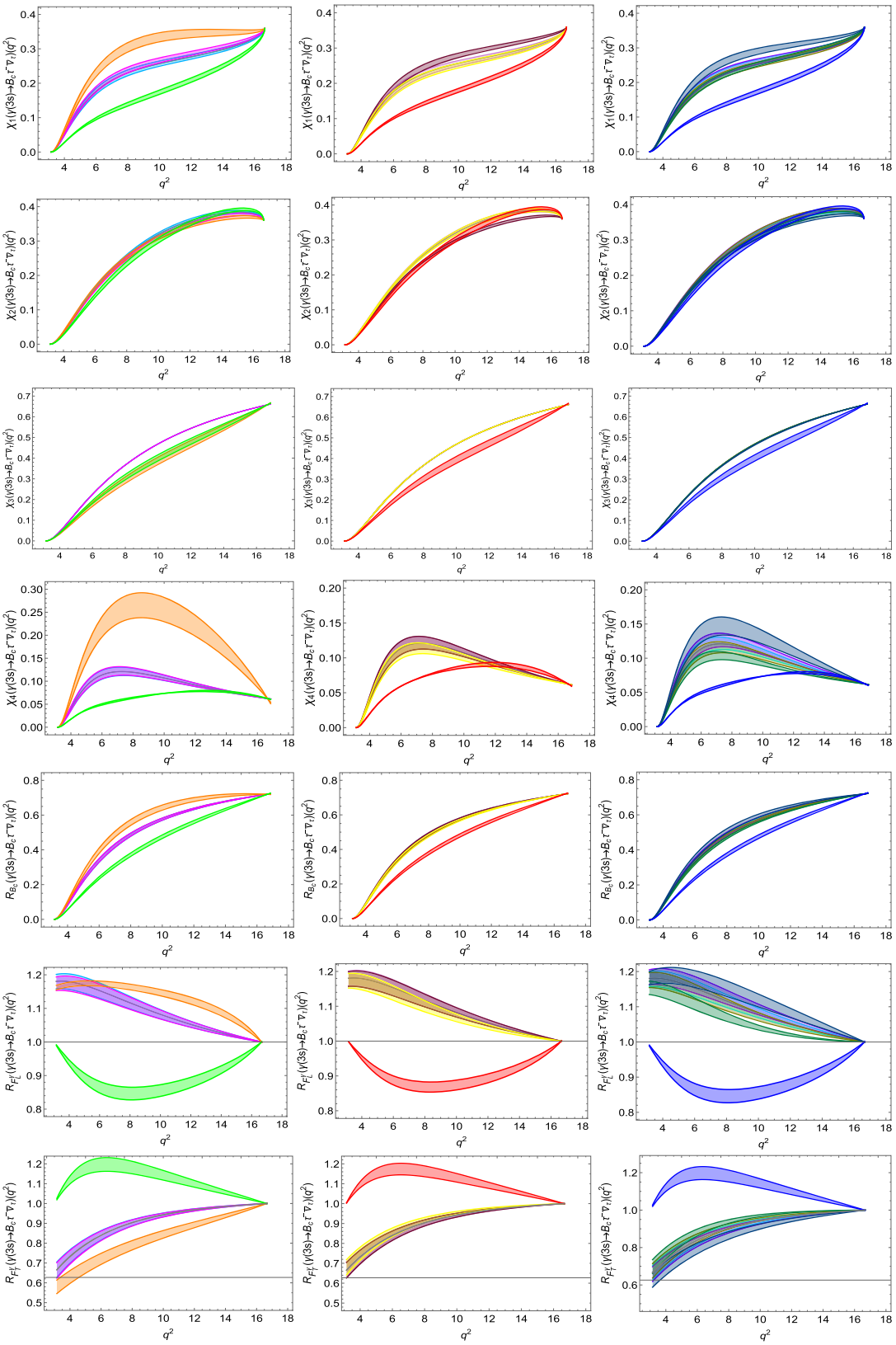

Fig. 5 The q^2 distributions of the observables $\chi_{1(2,3,4)}(q^2)$, and $R_{B_c}(q^2)$ as well as $R_{F_{L(T)}^{\Upsilon}}(q^2)$ for the decays $\Upsilon(3S) \to B_c \tau \bar{\nu}_\tau$ in the SM, case A (left column), case B (middle column), case C (right column) NP scenarios, respectively

coupling in BMP4, BMP8, BMP13 and BMP14 scenarios. However, significant decrease effect appears in $A_{FB}(q^2)$, $C_F^\tau(q^2)$, $F_L^\Upsilon(q^2)$ for lower q^2 region and in $\chi_{1,3,4}(q^2)$, $R_{B_c}(q^2)$ and $R_{F_L^\Upsilon}(q^2)$ for entail q^2 region after considering the NP parameters in BMP4, BMP8 and BMP14 scenarios. And significant enhancement effect also appears in $F_T^\Upsilon(q^2)$, $P_\tau(q^2)$ and $R_{F_L^\Upsilon}(q^2)$ in the reasonable kinematic region in BMP4, BMP8 and BMP14 scenarios. Though it is clear to find that there is an axial symmetric phenomenon between $F_L^{\Upsilon(nS)}(q^2)$ and $F_T^{\Upsilon(nS)}(q^2)$ shown in Fig. 4, the same axial symmetric phenomenon does not occur in the $R_{F_T^\Upsilon}(q^2)$ and $R_{F_L^\Upsilon}(q^2)$ which is displayed in Fig. 5. In this work, for the various NP scenarios, we only consider the impact of hadronic form factor uncertainties on the errors of various observables., while ignoring the errors brough by the uncertainties of the different NP coupling parameters So these analysis is merely illustrative. With the continuous upgrading of the high energy physics experimental facilities in the future, there may be better improvements in the relevant decay processes.

Unlike B meson decays, which have been extensively investigated both experimentally and theoretically in the last few years, research on the $\Upsilon(nS)$ mesons remains very scarce, especially on the theoretical side. Although some observables studied above are very sensitive to NP effects within the NP scenarios, it is difficult to measure them soon because there are no effective techniques or methods to measure them directly under current experimental conditions. Since hadronic decays involving $b \to c$ transitions play a significate role in heavy flavor physics experiments, this work is very crucial to research such decay modes. The exploration of these decays is also beneficial for the study of charmed hadron decays. The research on the $\Upsilon(nS)$ mesons in this work would be found to be very important in shedding light on the nature of NP. The existence of the NP signal that contributes to the heavy flavor sector is expected to be discovered in the era of precision measurements. Therefore, the study of semileptonic decays of the $\Upsilon(nS)$ mesons will not only contribute to a better understanding of heavy flavor physics but also provide a good environment for the search of NP signal in the future.

Acknowledgements This work was supported by the National Natural Science Foundation of China (Contracts Nos. 12305100, 12365014 and 12175088). J.H Sheng is also supported by the Key Scientific Research Projects of Colleges and Universities in Henan Province (Contract No. 24B140003). F.Z Zhou is supported by the Key R. & D. Promotion Project of Henan Province (No. 222102240018)

Data Availability Statement This manuscript has no associated data. [Author's comment: All data generated during this study are already contained in this published paper.]

Code Availability Statement The manuscript has no associated code/software. [Author's comment: Code/software will be made available on reasonable request.]

Funded by SCOAP[3].

References

1. F.M. Bhutta, N. Farooq, Z.R. Huang, Y. Li, M.A. Paracha, Reinvestigating the semileptonic $B \to D^{(*)}\tau\bar{\nu}_\tau$ decays in the model independent scenarios and leptoquark models. https://inspirehep.net/literature/2865816. arXiv:2501.03734 [hep-ph]
2. R. Watanabe, New physics effect on $B_c \to J/\psi\tau\bar{\nu}$ in relation to the $R_{D^{(*)}}$ anomaly. Phys. Lett. B **776**, 5–9 (2018) https://inspirehep.net/literature/1625754
3. D. Leljak, B. Melic, M. Patra, On lepton flavour universality in semileptonic $B_c \to \eta_c(J\psi)$, decays. JHEP **05**, 094 (2019) https://inspirehep.net/literature/1716582
4. C.T. Tran, M.A. Ivanov, Implications of new physics in the decays $B_c \to (J/\psi, \eta_c)\tau\nu$. Phys. Rev. D **97**(5), 054014 (2018) https://inspirehep.net/literature/1649208
5. S. Khan, D. Kumar, New physics effects in semileptonic $\bar{B}_s \to K^{*+}(\to K\pi)\ell^-\bar{\nu}_\ell$ decay. arXiv:2411.03238 [hep-ph]
6. J.N. Pandya, P. Santorelli, N.R. Soni, Prediction of various observables for $B_s^0 \to D_s^{(*)-}\ell^+\nu_\ell$ within covariant confined quark model. https://inspirehep.net/literature/2681725. arXiv:2307.14245 [hep-ph]
7. S. Sahoo, A. Bhol, Efficacy of scalar leptoquark on $B_s \to K^{(*)}\tau\bar{\nu}_\tau$ decay modes. https://inspirehep.net/literature/1797887. arXiv:2005.12630 [hep-ph]
8. S.W. Wang, Probing the effects of some new physics models in $B_s \to D_s\tau\bar{\nu}$ decay. Nucl. Phys. B **954**, 114997 (2020) https://inspirehep.net/literature/1789728
9. S. Sahoo, R. Mohanta, Investigating the role of new physics in $b \to c\tau\bar{\nu}_\tau$ transitions. https://inspirehep.net/literature/1759920. arXiv:1910.09269 [hep-ph]
10. A. Ray, S. Sahoo, R. Mohanta, Model independent analysis of $B^* \to P\ell\bar{\nu}_\ell$ decay processes. Eur. Phys. J. C **79**(8), 670 (2019) https://inspirehep.net/literature/1747271
11. J. Zhang, Y. Zhang, Q. Zeng, R. Sun, New physics effects of the vector leptoquark on $\bar{B}^* \to P\tau\bar{\nu}_\tau$ decays. Eur. Phys. J. C **79**(2), 164 (2019)
12. Q. Chang, J. Zhu, X.L. Wang, J.F. Sun, Y.L. Yang, Study of semileptonic $\Upsilon(nS) \to B_c\ell\bar{\nu}_\ell$ weak decays. J. Phys. G **44**(1), 015001 (2017) https://inspirehep.net/literature/1502248
13. Q. Chang, J. Zhu, N. Wang, R.M. Wang, Probing the effects of new physics in $\bar{B}^* \to P\ell\bar{\nu}_\ell$ decays. Adv. High Energy Phys. **2018**, 7231354 (2018) https://inspirehep.net/literature/1685387
14. J.H. Sheng, J. Zhu, Q.Y. Hu, Investigation on the new physics effects of the vector leptoquark on semileptonic $\bar{B}^* \to V\tau^-\bar{\nu}_\tau$

decays. Eur. Phys. J. C **81**(6), 524 (2021) https://inspirehep.net/literature/1869634
15. Q. Chang, J. Zhu, X.L. Wang, J.F. Sun, Y.L. Yang, Study of semileptonic $B^* \to Pl\bar{\nu}_l$decays. Nucl. Phys. B **909**, 921–933 (2016) https://inspirehep.net/literature/1472243
16. J.H. Sheng, Q.Y. Hu, R.M. Wang, J. Zhu, Phenomenology analysis of $\bar{B}^* \to V\tau^-\bar{\nu}_\tau$ decays in and beyond the Standard Model. Eur. Phys. J. C **82**(8), 768 (2022) https://inspirehep.net/literature/2146126
17. R. Dutta, A. Bhol, A.K. Giri, Effective theory approach to new physics in $b \to u$ and $b \to c$ leptonic and semileptonic decays. Phys. Rev. D **88**(11), 114023 (2013) https://inspirehep.net/literature/1244532
18. A. Datta, S. Kamali, S. Meinel, A. Rashed, Phenomenology of $\Lambda_b \to \Lambda_c\tau\bar{\nu}_\tau$ using lattice QCD calculations. JHEP **08**, 131 (2017) https://inspirehep.net/literature/1512597
19. X.L. Mu, Y. Li, Z.T. Zou, B. Zhu, Investigation of effects of new physics in $\Lambda_b \to \Lambda_c\tau\bar{\nu}_\tau$ decay. Phys. Rev. D **100**(11), 113004 (2019) https://inspirehep.net/literature/1755653
20. X.Q. Li, Y.D. Yang, X. Zhang, Revisiting the one leptoquark solution to the R(D$^{(*)}$) anomalies and its phenomenological implications. JHEP **08**, 054 (2016) https://inspirehep.net/literature/1466323
21. S. Nandi, S. Sahoo, R. Sain, An Imperative study of the angular observables in $\Lambda_b^0 \to \Lambda_c^+(\to \Lambda\pi^+)\tau\bar{\nu}_\tau$ decay and probing the footprint of new physics. https://inspirehep.net/literature/2769929. arXiv:2403.12155 [hep-ph]
22. S. Karmakar, S. Chattopadhyay, A. Dighe, Identifying physics beyond SMEFT in the angular distribution of $\Lambda_b \to \Lambda_c(\Lambda\pi)\tau\bar{\nu}_\tau$ decay. Phys. Rev. D **110**(1), 015010 (2024) https://inspirehep.net/literature/2662636
23. R. Dutta, $\Lambda_b \to (\Lambda_c,\ p)\,\tau\,\nu$ decays within standard model and beyond. Phys. Rev. D **93**(5), 054003 (2016) https://inspirehep.net/literature/1409518
24. A. Ray, S. Sahoo, R. Mohanta, Probing new physics in semileptonic Λ_b decays. Phys. Rev. D **99**(1), 015015 (2019) https://inspirehep.net/literature/1710392
25. S. Shivashankara, W. Wu, A. Datta, $\Lambda_b \to \Lambda_c\tau\bar{\nu}_\tau$ decay in the Standard Model and with new physics. Phys. Rev. D **91**(11), 115003 (2015) https://inspirehep.net/literature/1346412
26. T. Gutsche, M.A. Ivanov, J.G. Korner, V.E. Lyubovitskij, P. Santorelli, N. Habyl, Semileptonic decay $\Lambda_b \to \Lambda_c\tau^-\bar{\nu}_\tau$ in the covariant confined quark model. Phys. Rev. D **91**(7), 074001 (2015) https://inspirehep.net/literature/1345174
27. H.W. Ke, N. Hao, X.Q. Li, Revisiting $\Lambda_b \to \Lambda_c$ and $\Sigma_b \to \Sigma_c$ weak decays in the light-front quark model. Eur. Phys. J. C **79**(6), 540 (2019) https://inspirehep.net/literature/1729308
28. J. Zhang, X. An, R. Sun, J. Su, Probing new physics in semileptonic $\Xi_b \to \Lambda(\Xi_c)\tau^-\bar{\nu}_\tau$ decays. Eur. Phys. J. C **79**(10), 863 (2019) https://inspirehep.net/literature/1761658
29. J. Zhang, J. Su, Q. Zeng, Contributions of vector leptoquark to $\Xi_b \to \Xi_c\tau\nu_\tau$ decay. Nucl. Phys. B **938**, 131–142 (2019) https://inspirehep.net/literature/1704249
30. R. Dutta, Phenomenology of $\Xi_b \to \Xi_c\,\tau\,\nu$ decays. Phys. Rev. D **97**(7), 073004 (2018) https://inspirehep.net/literature/1646697
31. H.W. Ke, X.H. Yuan, X.Q. Li, Z.T. Wei, Y.X. Zhang, $\Sigma_b \to \Sigma_c$ and $\Omega_b \to \Omega_c$ weak decays in the light-front quark model. Phys. Rev. D **86**, 114005 (2012) https://inspirehep.net/literature/1122675
32. H.W. Ke, N. Hao, X.Q. Li, $\Sigma_b \to \Sigma_c^*$ weak decays in the light-front quark model with two schemes to deal with the polarization of diquark. J. Phys. G **46**(11), 115003 (2019) https://inspirehep.net/literature/1634868
33. N. Rajeev, R. Dutta, S. Kumbhakar, Implication of $R_{D^{(*)}}$ anomalies on semileptonic decays of Σ_b and Ω_b baryons. Phys. Rev. D **100**(3), 035015 (2019) https://inspirehep.net/literature/1737630
34. J.H. Sheng, J. Zhu, X.N. Li, Q.Y. Hu, R.M. Wang, Probing new physics in semileptonic Σ_b and Ω_b decays. Phys. Rev. D **102**(5), 055023 (2020) https://inspirehep.net/literature/1818174
35. J.H. Sheng, Q.Y. Hu, J. Zhu, Investigation of the effects of some new physics models in semileptonic Ξ_b and Ω_b decays. J. Phys. G **49**(1), 015001 (2022) https://inspirehep.net/literature/1983355
36. Mk. Du, C. Liu, Ω_b semi-leptonic weak decays. Phys. Rev. D **84**, 056007 (2011) https://inspirehep.net/literature/918278
37. S.W. Herb et al., Observation of a dimuon resonance at 9.5-GeV in 400-GeV proton-nucleus collisions. Phys. Rev. Lett. **39**, 252–255 (1977) https://inspirehep.net/literature/120368
38. W.R. Innes et al., Observation of structure in the Υ region. Phys. Rev. Lett. **39**, 1240–1242 (1977) https://inspirehep.net/literature/121100
39. Citation: S. Navas et al., (Particle Data Group), Phys. Rev. D110, 030001 (2024). https://inspirehep.net/literature/2817040
40. M.A. Sanchis-Lozano, On the search for weak decays of heavy quarkonium in dedicated heavy quark factories. Z. Phys. C **62**, 271–280 (1994) https://inspirehep.net/literature/362378
41. Y.M. Wang, H. Zou, Z.T. Wei, X.Q. Li, C.D. Lu, The transition form-factors for semi-leptonic weak decays of J/ψ in QCD sum rules. Eur. Phys. J. C **54**, 107–121 (2008) https://inspirehep.net/literature/755274
42. Y.M. Wang, H. Zou, Z.T. Wei, X.Q. Li, C.D. Lu, Weak decays of J/ψ: the non-leptonic case. Eur. Phys. J. C **55**, 607–613 (2008) https://inspirehep.net/literature/779743
43. Y.M. Wang, H. Zou, Z.T. Wei, X.Q. Li, C.D. Lu, FCNC-induced semileptonic decays of J/ψ in the Standard Model. J. Phys. G **36**, 105002 (2009) https://inspirehep.net/literature/800039
44. Y.L. Shen, Y.M. Wang, J/ψ weak decays in the covariant light-front quark model. Phys. Rev. D **78**, 074012 (2008) https://inspirehep.net/literature/800370
45. H.W. Ke, Y.Z. Chen, X.Q. Li, The decay rate of $J/\psi \to \Lambda_c + \bar{\Sigma}^+$ in SM and beyond. Chin. Phys. Lett. **28**, 071301 (2011) https://inspirehep.net/literature/890858
46. J. Sun, L. Chen, Q. Chang, J. Huang, Y. Yang, $J/\psi \to DP, DV$ decays in the QCD factorization approach. Int. J. Mod. Phys. A **30**(16), 1550094 (2015) https://inspirehep.net/literature/1383551
47. J. Sun, Y. Yang, J. Gao, Q. Chang, J. Huang, G. Lu, $J/\psi \to D_{s,d}\pi, D_{s,d}K$ decays with perturbative QCD approach. Phys. Rev. D **94**(3), 034029 (2016) https://inspirehep.net/literature/1623903
48. Y. Yang, J. Sun, J. Gao, Q. Chang, J. Huang, G. Lu, Study of $J/\psi \to D_{s,d}V$ decays with perturbative QCD approach. Int. J. Mod. Phys. A **31**(30), 1650161 (2016) https://inspirehep.net/literature/1496130
49. J. Sun, Q. Li, Y. Yang, H. Li, Q. Chang, Z. Zhang, $\Upsilon(1S) \to B_c\pi, B_cK$ decays with perturbative QCD approach. Phys. Rev. D **92**(7), 074028 (2015) https://inspirehep.net/literature/1400385
50. J. Sun, Y. Yang, Q. Li, H. Li, N. Wang, Q. Chang, J. Huang, Study on the $\Upsilon(1S) \to B_cD_s$ decay. Nucl. Phys. B **903**, 374–386 (2016) https://inspirehep.net/literature/1415078
51. J. Sun, Y. Yang, Q. Li, H. Li, Q. Chang, J. Huang, The $\Upsilon(1S) \to B_c\rho$ decay with perturbative QCD approach. Nucl. Phys. B **909**, 186–196 (2016) https://inspirehep.net/literature/1412079
52. J. Sun, Y. Yang, Q. Li, G. Lu, J. Huang, Q. Chang, Study of the $\Upsilon(1S) \to B_cD_s^*$ decay with pQCD approach. Int. J. Mod. Phys. A **31**(12), 1650061 (2016) https://inspirehep.net/literature/1451776
53. J. Sun, L. Chen, N. Wang, Q. Chang, J. Huang, Y. Yang, Study on the $\Upsilon(1S) \to B_cM$ weak decays. Adv. High Energy Phys. **2015**, 691261 (2015) https://inspirehep.net/literature/1387833
54. Hn. Li, Applicability of perturbative QCD to B –> D decays. Phys. Rev. D **52**, 3958–3965 (1995)
55. C.H.V. Chang, Hn. Li, Three-scale factorization theorem and effective field theory. Phys. Rev. D **55**, 5577–5580 (1997) https://inspirehep.net/literature/420266

56. T.W. Yeh, Hn. Li, Factorization theorems, effective field theory, and nonleptonic heavy meson decays. Phys. Rev. D **56**, 1615–1631 (1997) https://inspirehep.net/literature/439443
57. M. Beneke, G. Buchalla, M. Neubert, C.T. Sachrajda, QCD factorization for $B \to \pi\pi$ decays: strong phases and CP violation in the heavy quark limit. Phys. Rev. Lett. **83**, 1914–1917 (1999) https://inspirehep.net/literature/499707
58. M. Beneke, G. Buchalla, M. Neubert, C.T. Sachrajda, QCD factorization for exclusive, nonleptonic B meson decays: general arguments and the case of heavy light final states. Nucl. Phys. B **591**, 313–418 (2000) https://inspirehep.net/literature/528680
59. J. Sun, L. Chen, N. Wang, J. Huang, Y. Yang, Q. Chang, Study on $\Upsilon(nS) \to B_c M$ decays. J. Phys. G **42**(10), 105005 (2015) https://inspirehep.net/literature/1393873
60. J. Sun, Y. Yang, Q. Li, H. Li, Q. Chang, J. Huang, The $\Upsilon(nS) \to B_c D_s$, $B_c D_d$ decays with perturbative QCD approach. Phys. Lett. B **752**, 322–328 (2016) https://inspirehep.net/literature/1649150
61. Q. Chang, Y. Zhang, L. Han, Study of $\Upsilon(nS) \to B_c \rho$ and $B_c K^*$ decays within the QCD factorization. Mod. Phys. Lett. A **31**(38), 1650209 (2016) https://inspirehep.net/literature/1501183
62. J. Sun, Y. Yang, J. Huang, G. Lu, Q. Chang, $\Upsilon(nS) \to B_c \rho B_c K$ decays with perturbative QCD approach. Nucl. Phys. B **911**, 890–901 (2016) https://inspirehep.net/literature/1486146
63. Y. Yang, J. Sun, Y. Guo, Q. Li, J. Huang, Q. Chang, Study of $\Upsilon(nS) \to B_c P$ decays with perturbative QCD approach. Phys. Lett. B **751**, 171–176 (2015) https://inspirehep.net/literature/1400888
64. K.K. Sharma, R.C. Verma, Rare decays of ψ and Υ. Int. J. Mod. Phys. A **14**, 937–946 (1999) https://inspirehep.net/literature/466005
65. A.J. Bevan et al., [BaBar and Belle], The Physics of the B Factories. Eur. Phys. J. C **74**, 3026 (2014). https://inspirehep.net/literature/1302816
66. SuperKEKB Project (https://www-superkekb.kek.jp/)
67. M. Ablikim et al., [BESIII], Search for the semi-muonic charmonium decay $J/\psi \to D^- \mu^+ \nu_\mu$. JHEP **01** (2024), 126. https://inspirehep.net/literature/2674357
68. M. Ablikim et al., [BESIII], Search for the rare semi-leptonic decay $J/\psi \to D^- e^+ \nu_e + c.c.$ JHEP **06**, 157 (2021). https://inspirehep.net/literature/1858267
69. M.A. Ivanov, C.T. Tran, Exclusive decays $J/\psi \to D_{(s)}^{(*)-} l^+ \nu_l$ in a covariant constituent quark model with infrared confinement. Phys. Rev. D **92**(7), 074030 (2015) https://inspirehep.net/literature/1400382
70. T. Wang, Y. Jiang, H. Yuan, K. Chai, G.L. Wang, Weak decays of J/ψ and $\Upsilon(1S)$. J. Phys. G **44**(4), 045004 (2017) https://inspirehep.net/literature/1445115
71. R. Dhir, R.C. Verma, Effects of flavor dependence on weak decays of J/ψ and Υ. Adv. High Energy Phys. **2013**, 706543 (2013) https://inspirehep.net/literature/814884
72. V. Cirigliano, J. Jenkins, M. Gonzalez-Alonso, Semileptonic decays of light quarks beyond the Standard Model. Nucl. Phys. B **830**, 95–115 (2010) https://inspirehep.net/literature/828381
73. T. Bhattacharya et al., Probing novel scalar and tensor interactions from (Ultra) cold neutrons to the LHC. Phys. Rev. D **85**, 054512 (2012) https://inspirehep.net/literature/943731
74. A. Kadeer, J.G. Korner, U. Moosbrugger, Helicity analysis of semileptonic hyperon decays including lepton mass effects. Eur. Phys. J. C **59**, 27–47 (2009) https://inspirehep.net/literature/696766
75. J.G. Korner, G.A. Schuler, Exclusive semileptonic heavy meson decays including lepton mass effects. Z. Phys. C **46**, 93 (1990) https://inspirehep.net/literature/282092
76. C. Murgui, A. Pe nuelas, M. Jung, A. Pich, Global fit to $b \to c\tau\nu$ transitions. JHEP **09**, 103 (2019). https://inspirehep.net/literature/1730526
77. Q.Y. Hu, X.Q. Li, Y.D. Yang, $b \to c\tau\nu$ transitions in the standard model effective field theory. Eur. Phys. J. C **79**(3), 264 (2019) https://inspirehep.net/literature/1698008
78. C. Bobeth, G. Hiller, D. van Dyk, The benefits of $\bar{B} \to \bar{K}^* l^+ l^-$ decays at low recoil. JHEP **07**, 098 (2010) https://inspirehep.net/literature/859520
79. CKMfitter Group CKMfitter global fit results as of Spring 21. http://ckmfitter.in2p3.fr/www/results/plots_spring21/num/ckmEval_results_spring21.html
80. M. Wirbel, B. Stech, M. Bauer, Exclusive semileptonic decays of heavy mesons. Z. Phys. C **29**, 637 (1985) https://inspirehep.net/literature/218136
81. M. Bauer, M. Wirbel, Form-factor effects in exclusive d and B decays. Z. Phys. C **42**, 671 (1989) https://inspirehep.net/literature/24229
82. C.T. Tran, M.A. Ivanov, P. Santorelli, H.C. Tran, Study of the semileptonic decays $\Upsilon(1S) \to B_{(c)} \ell \bar{\nu}_\ell$. arXiv:2408.13776 [hep-ph]. https://inspirehep.net/literature/2821756
83. X. Q. Li, X. Xu, Y.D. Yang, D.H. Zheng, $B_c^- \to J/\psi \left(\to \mu^+\mu^-\right) \tau^- \left(\to \pi^-\nu_\tau, \rho^-\nu_\tau, \ell^-\bar{\nu}_\ell\nu_\tau\right)\bar{\nu}_\tau$ decays with visible final-state kinematics. JHEP **05**, 173 (2023). https://inspirehep.net/literature/2636772
84. J. Harrison et al., [HPQCD], $B_c \to J/\psi$ form factors for the full q^2 range from lattice QCD. Phys. Rev. D **102**(9), 094518 (2020). https://inspirehep.net/literature/1806790
85. S.Y. Wang, Y.Y. Yang, Z.J. Sun, H. Yang, P. Li, Z.Q. Zhang, Semileptonic and nonleptonic decays of $\boldsymbol{B}^*_{\boldsymbol{u,d,s}}$ in the covariant light-front approach. Chin. Phys. C **48**(12), 123102 (2024). https://doi.org/10.1088/1674-1137/ad7247
86. M. Blanke, A. Crivellin, T. Kitahara, Addendum to "Impact of polarization observables and $B_c \to \tau\nu$ on new physics explanations of the $b \to c\tau\nu$ anomaly. Phys. Rev. D **100**(3), 035035 (2019) https://inspirehep.net/literature/1735859
87. K. Cheung, Z.R. Huang, H.D. Li, C.D. Lü, Y.N. Mao, R.Y. Tang, Revisit to the $b \to c\tau\nu$ transition: In and beyond the SM. Nucl. Phys. B **965**, 115354 (2021) https://inspirehep.net/literature/1781286
88. A.K. Alok, D. Kumar, J. Kumar, S. Kumbhakar, S.U. Sankar, New physics solutions for R_D and R_{D^*}. JHEP **09**, 152 (2018) https://inspirehep.net/literature/1629972
89. A.K. Alok, D. Kumar, S. Kumbhakar, S.U. Sankar, Solutions to R_D-R_{D^*} in light of Belle 2019 data. Nucl. Phys. B **953**, 114957 (2020) https://inspirehep.net/literature/1726539
90. M. Blanke, A. Crivellin, S. de Boer, T. Kitahara, M. Moscati, U. Nierste, I. Nis and zic, Impact of polarization observables and $B_c \to \tau\nu$ on new physics explanations of the $b \to c\tau\nu$ anomaly. Phys. Rev. D **99**(7), 075006 (2019). https://inspirehep.net/literature/1704733
91. M. Arslan, T. Yasmeen, S. Shafaq, I. Ahmed, M.J. Aslam, Analysis of anomalies using weak effective Hamiltonian with complex couplings and their impact on various physical observables. Chin. Phys. C **48**(8), 083103 (2024) https://inspirehep.net/literature/2698782
92. C.P. Haritha, K. Jain, B. Mawlong, Analysis of some $b \to c\tau\bar{\nu}_\tau$ decay modes beyond the standard model. Nucl. Phys. B **994**, 116309 (2023) https://inspirehep.net/literature/2696447
93. C.P. Haritha, K. Jain, B. Mawlong, Semileptonic b-baryon decays within a new physics approach. Eur. Phys. J. C **83**(2), 136 (2023) https://inspirehep.net/literature/2631337